



# Synthesis of organometallic Ru(II) and Fe(II) complexes containing fused rings hemi-helical ligands as chromophores. Evaluation of non-linear optical properties by HRS

M. Helena Garcia<sup>a,\*</sup>, Pedro Florindo<sup>a</sup>, M. Fátima M. Piedade<sup>b</sup>, M. Teresa Duarte<sup>b</sup>, M. Paula Robalo<sup>b,c</sup>, Jürgen Heck<sup>d</sup>, Christian Wittenburg<sup>d</sup>, Jan Holtmann<sup>d</sup>, Emanuela Licandro<sup>e</sup>

<sup>a</sup>Centro de Ciências Moleculares e Materiais, Faculdade de Ciências da Universidade de Lisboa, Edifício C8, Campo Grande, 1749-016 Lisboa, Portugal

<sup>b</sup>Centro de Química Estrutural, Instituto Superior Técnico, Universidade Técnica de Lisboa, Av. Rovisco Pais, 1049-001 Lisboa, Portugal

<sup>c</sup>Departamento de Engenharia Química, Instituto Superior de Engenharia de Lisboa, Rua Conselheiro Emídio Navarro, 1, 1959-007 Lisboa, Portugal

<sup>d</sup>Institut für Anorganische und Angewandte Chemie, Universität Hamburg, Martin-Luther-King-Platz 6, D-20146 Hamburg, Germany

<sup>e</sup>Dipartimento di Chimica Organica e Industriale, Università degli Studi di Milano, Via C. Golgi, 19, 20133 Milano, Italy

## ARTICLE INFO

### Article history:

Received 4 April 2008

Received in revised form 7 May 2008

Accepted 7 May 2008

Available online 31 July 2008

Dedicated to the memory of Professor Alberto Romão Dias.

### Keywords:

Ruthenium(II)

Iron(II)

Benzodithiophene

Nonlinear optics

Hyper-Rayleigh scattering (HRS)

Monocyclopentadienyl complexes

## ABSTRACT

A new family of three-legged piano stool structured organometallic compounds containing the fragment  $\eta^5$ -cyclopentadienyl-ruthenium(II)/iron(II) has been synthesized to evaluate the existence of electronic metal to ligand charge transfer upon coordination of the novel benzodithiophene ligands (**BDT**), benzo[1,2-*b*;4,3-*b'*]dithiophen-2-carbonitrile (**L1**) and benzo[1,2-*b*;4,3-*b'*]dithiophen-2-nitro-2-carbonitrile (**L2**). All the compounds were characterized by <sup>1</sup>H, <sup>13</sup>C, <sup>31</sup>P NMR, IR and UV–Vis. spectroscopies and their electrochemistry studied by cyclic voltammetry. The X-ray structures of [Ru( $\eta^5$ -C<sub>5</sub>H<sub>5</sub>)(PPh<sub>3</sub>)<sub>2</sub>-(NCC<sub>10</sub>H<sub>5</sub>S<sub>2</sub>)] [PF<sub>6</sub>] (**1Ru**), [Ru( $\eta^5$ -C<sub>5</sub>H<sub>5</sub>)(PPh<sub>3</sub>)<sub>2</sub>(NCC<sub>10</sub>H<sub>5</sub>S<sub>2</sub>)] [CF<sub>3</sub>SO<sub>3</sub>] (**1' Ru**), [Ru( $\eta^5$ -C<sub>5</sub>H<sub>5</sub>)(DPPE)(NCC<sub>10</sub>-H<sub>5</sub>S<sub>2</sub>)] [PF<sub>6</sub>] (**2Ru**) and [Fe( $\eta^5$ -C<sub>5</sub>H<sub>5</sub>)(DPPE)(NCC<sub>10</sub>H<sub>5</sub>S<sub>2</sub>)] [PF<sub>6</sub>] (**2Fe**) were determined by X-ray diffraction showing centric crystallization on groups P1 and P2<sub>1</sub>/n, respectively.

Quadratic hyperpolarizabilities ( $\beta$ ) of some of the complexes (**2Fe**, **2Ru** and **3Fe**) have been determined by hyper-Rayleigh scattering (HRS) measurements at a fundamental wavelength of 1500 nm, to minimize the probability of fluorescence due to two-photon absorption and to reduce the effect of resonance enhancement, in order to estimate static  $\beta$  values.

© 2008 Elsevier B.V. All rights reserved.

## 1. Introduction

The search for new organometallic materials with nonlinear optical (NLO) properties has been an area of considerable interest due to its relevance to optical device technology [1–6].

The high values of first molecular hyperpolarizability ( $\beta$ ) found in organometallic compounds has been related to low energy electronic metal-to-ligand or ligand-to-metal charge transfer excitations. In addition, this charge transfer energy can be tuned by variation of the metal itself and its oxidation state, ligand environment and coordination geometries in order to optimize the second order NLO response. Significant results have been achieved in push–pull systems in which the metal centre, bonded to a polarizable organic conjugated backbone (chromophore), acts as an electron releasing or withdrawing group [1–6]. In particular, structures presenting the metal centre and the chromophore in the same

plane, have been found of potential interest for second-order optical nonlinearities, due to the charge delocalization through a  $d_{\text{metal}}-\pi_{\text{ligand}}^*$  interaction. This is widely illustrated in the literature by the families of  $\eta^5$ -monocyclopentadienyl iron and ruthenium molecular materials presenting *p*-nitrobenzonitriles [7–10], *p*-nitrobenzoacetylides [11–13], nitrothienylacetylides [14] and thiophene derivatives [15].

Although the first molecular hyperpolarizability of purely organic push–pull molecules increases strongly with the length of the conjugated chain [16,17], this is not the case for the benzoderivatives, due to the torsion angle between the rings. Nevertheless, the extension of conjugation turns out effective by insertion of a vinylene unit between two phenyl rings. Yet, extended conjugated chain in systems based on thiophene rings, is expected to present an improved planarity since the torsion angle between rings can become quite small. In accordance, *ab initio* calculations [18] suggests that for terthiophene, although the gas-phase structure is not planar, the conformational inter-conversion energy is very low and sensitive to the chemical environment. Also a

\* Corresponding author. Tel.: +351 217500972; fax: +351 217500088.

E-mail addresses: lena.garcia@ist.utl.pt, i017@alfa.ist.utl.pt (M.H. Garcia).

semi-empirical calculation, indicating that the structure of bithiophene becomes planar in water solution [19], supports the assumption of easier planarity on oligothiophene compounds.

Our recent studies in complexes containing the organometallic donor fragment  $[\text{FeCp}(\text{P-P})]^+$  ( $\text{P-P} = \text{DPPE}, (+)\text{-DIOP}$ ) and conjugated thiophene derived ligands, showed an improved electronic  $\pi$ -coupling between the  $\eta^5$ -cyclopentadienyl iron fragment and the  $\pi$ -system of the conjugated thiophene ligands, when compared to the previously reported *p*-benzonitrile analogues [15]. As a result, the first hyperpolarizabilities at 1.064  $\mu\text{m}$  are indeed higher than for the related benzonitrile compounds, and they could be scaled up by increasing the conjugation length, leading to the high  $\beta$   $910 \times 10^{-30}$  esu for the complex with three thiophene units. Nevertheless, the increased conjugation originated by that chain-lengthening can also be on the basis of a lowering of the charge-transfer (CT) efficiency, as was suggested by our published electrochemical and spectroscopic experimental data and also by the solvatochromic studies. The constancy of  $\beta_0 \sim 100 \times 10^{-30}$  esu upon chain-lengthening is a consequence of the compensation of two favourable effects, namely the increasing of conjugation length and the lowering of the charge transfer efficiency [15].

Therefore, it seems that the exploitation of promising thiophene based ligands for NLO purposes, should not be limited to the chain lengthening alternative, within this family of organometallic compounds, but instead, other alternatives seem to be quite pertinent.

In this work we explore the potentialities of new benzo[1,2-*b*;4,3-*b'*]dithiophene based chromophores where the fused rings structure guarantees the rigidity of the ligand to be coordinated on the same plan of the metal centre, in a family of cyclopentadienyl iron/ruthenium derivatives.

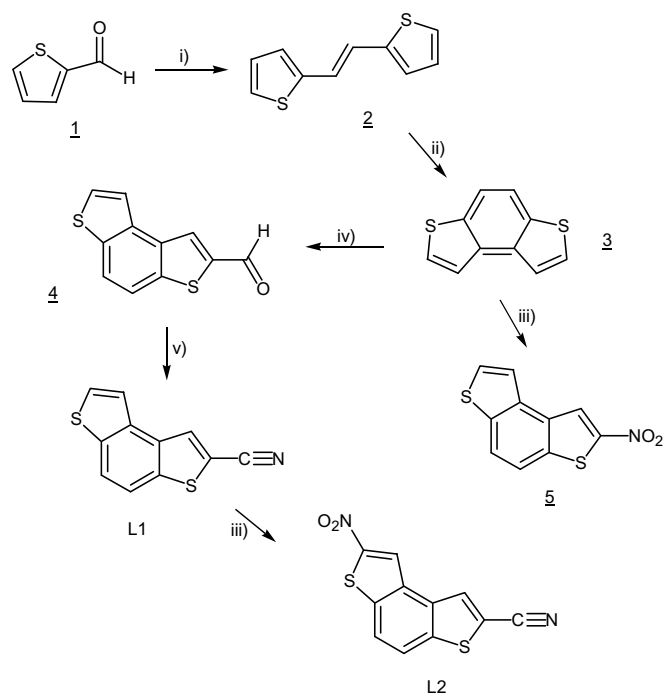
Although some reports concerning the NLO properties of thiophene-based organometallic complexes have been published, they are mainly about ferrocenyl and tricarbonyl chromium arene derivatives [20–26] in which the metal is unfavourably placed outside of the conjugation plane [27], in contrast with the present complexes and our previously reported oligothiophene containing complexes [15].

A new class of compounds for second-order NLO materials was developed, combining the organometallic donor fragment  $[\text{MCp}(\text{L}_L)]^+$ , ( $\text{M} = \text{Ru}(\text{II}), \text{L}_L = \text{DPPE}, 2\text{PPh}_3$  and  $\text{TMEDA}$ ;  $\text{M} = \text{Fe}(\text{II}), \text{L}_L = \text{DPPE}$ ) with the benzodithiophene functionalized molecules (**BDT**), namely benzo[1,2-*b*;4,3-*b'*]dithiophen-2-carbonitrile (**L1**) and benzo[1,2-*b*;4,3-*b'*]dithiophen-2'-nitro-2-carbonitrile (**L2**). The coligand  $\text{TMEDA}$  (*N,N,N',N'*-tetramethyl-ethylenediamine) was introduced in these studies to evaluate the ability of  $[\text{RuCp}(\text{TMEDA})]^+$  fragment as donor group comparatively to the well studied  $[\text{RuCp}(\text{P}_2)]^+$ . Spectroscopic and cyclic voltammetry data were analyzed to get some understanding about the electronic  $\pi$ -coupling between the  $\eta^5$ -cyclopentadienyliron/ruthenium fragment and the  $\pi$ -system of the benzodithiophene derived ligands. Quadratic hyperpolarizabilities of three compounds of this family have been determined by hyper-Rayleigh scattering (HRS) measurements at the fundamental wavelength of 1500 nm. These measurements revealed that the first hyperpolarizabilities are lower than expected.

## 2. Results and discussion

### 2.1. Synthesis of the benzodithiophene derived ligands (**BDT**)

The synthesis of the **BDT** ligands, benzo[1,2-*b*;4,3-*b'*]dithiophen-2-carbonitrile (**L1**) and benzo[1,2-*b*;4,3-*b'*]dithiophen-2'-nitro-2-carbonitrile (**L2**) is summarized in Scheme 1. The aldehyde starting material was prepared with good yield, by generation of the benzodithiophene  $\alpha$ -anion with *n*-BuLi and subsequent treatment with DMF, following Ref. [28].



- i) 1- dry THF,  $\text{TiCl}_4$ ,  $-20^\circ\text{C}$ ; 2- Zn dust, reflux; ii)  $h\nu$ ,  $\text{I}_2$ , air, toluene, r.t.; iii)  $\text{HNO}_3/\text{Ac}_2\text{O}$ ; iv) 1- dry THF,  $\text{N}_2$ ,  $-78^\circ\text{C}$ , *n*-BuLi; 2- DMF; v) 1-  $\text{H}_2\text{NOH}\cdot\text{HCl}$ , py,  $-30^\circ\text{C}$ ; 2-  $\text{Ac}_2\text{O}$ , reflux

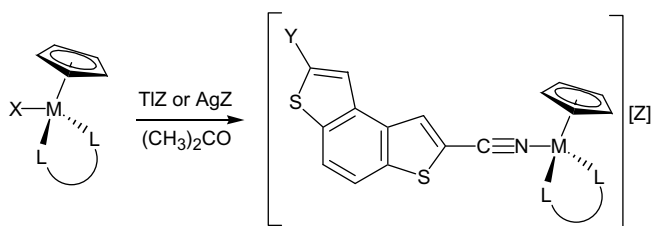
Scheme 1.

The new nitrile ligands, obtained with yields of 84% (**L1**) and 46% (**L2**), and the compounds **3** and **5**, were fully characterized by IR,  $^1\text{H}$  and  $^{13}\text{C}$  NMR spectroscopies and the elemental analysis were in accordance with the proposed formulations. The solid state FT-IR spectra (KBr pellets) showed the characteristic stretching vibration of the nitrile functional group at  $\sim 2215\text{ cm}^{-1}$  for both compounds. In addition, **L2** presented also the vibrations attributed to the  $\text{NO}_2$  group, at  $\sim 1515$  and  $1335\text{ cm}^{-1}$ .

### 2.2. Synthesis of the Ru(II)/Fe(II) complexes

Complexes of general formula  $[\text{M}(\eta^5\text{-C}_5\text{H}_5)(\text{LL})(\text{BDT})][\text{Z}]$ , with  $\text{Z} = \text{PF}_6^-$  and/or  $\text{CF}_3\text{SO}_3^-$ ; ( $\text{LL} = \text{DPPE}, 2\text{PPh}_3$  and  $\text{TMEDA}$  when  $\text{M} = \text{Ru}(\text{II})$  and ( $\text{LL} = \text{DPPE}$  when  $\text{M} = \text{Fe}(\text{II})$ );  $\text{BDT} = \text{benzo}[1,2\text{-}b;4,3\text{-}b']\text{dithiophen-2-carbonitrile}$  ( $\text{Y} = \text{H}$ ) and  $\text{benzo}[1,2\text{-}b;4,3\text{-}b']\text{dithiophen-2'-nitro-2-carbonitrile}$  ( $\text{Y} = \text{NO}_2$ ), were prepared, as shown in Scheme 2, by halide abstraction with  $\text{TlPF}_6$  (or  $\text{AgCF}_3\text{SO}_3$ ) from the parent neutral complexes  $[\text{M}(\eta^5\text{-C}_5\text{H}_5)(\text{LL})\text{X}]$  ( $\text{M} = \text{Fe}(\text{II}), \text{X} = \text{I}$ ;  $\text{M} = \text{Ru}(\text{II}), \text{X} = \text{Cl}$ ), in acetone, in the presence of an adequate excess of the corresponding nitrile.

The reactions were carried out at reflux, stirring overnight under inert atmosphere. The compounds were recrystallized by slow diffusion of *n*-heptane or *n*-hexane in acetone or dichloromethane solutions, giving crystalline yellow or orange products. With the exception of compound  $[\text{Ru}(\eta^5\text{-C}_5\text{H}_5)(\text{TMEDA})(\text{NCC}_{10}\text{H}_5\text{S}_2)][\text{PF}_6]$  (**4Ru**), which was very air sensitive, all the compounds were fairly stable to air and moisture, either in the solid state or in solution and were obtained in good yields (70–90%). Attempts to characterize the iron analogue  $[\text{Fe}(\eta^5\text{-C}_5\text{H}_5)(\text{TMEDA})(\text{NCC}_{10}\text{H}_5\text{S}_2)][\text{PF}_6]$  were unsuccessful, due to the instability of the compound. The formulation of all the new compounds is supported by analytical data, FT-IR and  $^1\text{H}$ ,  $^{13}\text{C}$ ,  $^{31}\text{P}$  NMR spectroscopic data. The solid state FT-IR spectra (KBr pellets) of the complexes presented a large number of bands which identify the presence of the various coligands.



- 1Ru** M=Ru(II); (LL) = 2PPh<sub>3</sub>; Y=H; Z= PF<sub>6</sub>  
**1'Ru** M=Ru(II); (LL) = 2PPh<sub>3</sub>; Y=H; Z= CF<sub>3</sub>SO<sub>3</sub>  
**2Ru** M=Ru(II); (LL) = DPPE; Y=H; Z= PF<sub>6</sub>  
**2Fe** M=Fe(II); (LL) = DPPE; Y=H; Z= PF<sub>6</sub>  
**3Fe** M=Fe(II); (LL) = DPPE; Y=NO<sub>2</sub>; Z= PF<sub>6</sub>  
**4Ru** M=Ru(II); (LL) = TMEDA; Y=H; Z= PF<sub>6</sub>

Scheme 2.

Typical bands were used to confirm the presence of the cyclopentadienyl ligand ( $\approx 3060\text{ cm}^{-1}$ ), the PF<sub>6</sub><sup>-</sup> anion (840 and 560  $\text{cm}^{-1}$ ) the CF<sub>3</sub>SO<sub>3</sub><sup>-</sup> anion (1253  $\text{cm}^{-1}$ ) and the coordinated nitrile ( $\nu_{\text{NC}}$  from 2215 to 2190  $\text{cm}^{-1}$ ) in all the studied complexes. As observed before for other ruthenium and iron related compounds, negative shifts up to  $-20\text{ cm}^{-1}$  were found for  $\nu_{\text{NC}}$  by comparison to the corresponding values of the uncoordinated nitrile. This effect has been attributed to  $\pi$ -backdonation due to  $\pi$  bonding between the d orbitals of the metal and the  $\pi^*$  orbital of the nitrile group, this leading to a decreased N $\equiv$ C bond order [8].

<sup>1</sup>H NMR chemical shifts of the cyclopentadienyl ring are displayed in the characteristic range of monocationic ruthenium(II) and iron(II) complexes. The coordination of the BDT derived nitriles leads to a shielding of most of the protons, particularly the one bonded to the adjacent carbon of the NC group (H<sub>3</sub> in Fig. 1).

The upfield shift was more significant along the family **1Ru** to **3Fe**. For compound **1Ru**, with PPh<sub>3</sub> as coligands, a maintenance of the positions of the aromatic protons upon coordination of the ligand is observed, with exception of H<sub>3</sub>, for which a shift of  $-0.35\text{ ppm}$  was observed. Nevertheless, the analogous compound **2Ru**, with the better donating coligand DPPE replacing PPh<sub>3</sub>, showed a negative shift of  $-1.34\text{ ppm}$  for H<sub>3</sub> and also small negative shifts for all the protons of the BDT ligands (see Table 1).

The shielding effect on H<sub>3</sub> in the coordinated ligand, became more evident for the iron analogue **2Fe**, for which H<sub>3</sub> was shifted to higher field by 1.4 ppm, although the other protons suffered about the same shielding as the **2Ru** analogue. The electron withdrawing effect of NO<sub>2</sub> in compound **3Fe** causes clearly an electronic delocalization throughout the coordinated ligand. Comparison of the chemical shifts of **3Fe** and **2Fe** to the ones of the respective uncoordinated ligands **L1** and **L2**, showed that while the proton H<sub>3</sub>, adjacent to CN group, was shielded 1.12 ppm (**3Fe**) and 1.40 ppm (**2Fe**) the proton H<sub>10</sub>, adjacent to the NO<sub>2</sub> group, was

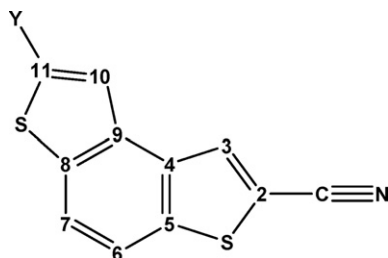


Fig. 1. Numbering scheme for NMR spectral assignments of Ru/Fe complexes and free BDT ligands.

Table 1

Selected <sup>1</sup>H NMR data for BDT ligands, free and coordinated to Ru/Fe organometallic fragments

Compound	Proton number					
	H <sub>11</sub>	H <sub>10</sub>	H <sub>7</sub>	H <sub>6</sub>	H <sub>3</sub>	Cp
<b>L1</b>	8.05	8.05	8.09	8.25	8.93	
<b>1Ru</b>	8.12	8.06	8.09	8.29	8.58	4.75
<b>1'Ru</b>	8.19	8.02	8.12	8.28	8.64	4.78
<b>2Ru</b>	8.07	7.86	7.93	8.19	7.59	4.99
<b>2Fe</b>	8.07	7.87	7.94	8.18	7.53	4.63
<b>4Ru</b>	8.05	8.05	8.12	8.25	8.94	4.54
<b>L2</b>		9.08	8.35	8.26	8.95	
<b>3Fe</b>		8.71	8.24	8.18	7.83	4.76

shielded 0.37 ppm in **3Fe**, and only 0.18 ppm in **2Fe**. The upfield shift of these protons, with special relevance for H<sub>10</sub>, indicates a shielding due to an electronic flow throughout the ligand towards the NO<sub>2</sub> electron withdrawing group, coming from the metal centre, due to a  $\pi$ -backdonation effect involving the coordinated nitrile group. This  $\pi$ -backdonation flow also confirmed by the NC stretching frequencies on the infrared spectra of all the compounds, was well illustrated by the negative shift of  $\sim -20\text{ cm}^{-1}$  observed for  $\nu_{\text{NC}}$  in compound **3Fe**. Nevertheless this effect of backdonation leads to an increased electronic density through the coordinated ligand only for compound **3Fe**, since for all the other compounds this effect was only relevant for the thiophene ring functionalised with the nitrile, i.e. the ring closest to the metal centre. Moreover, in the case of the TMEDA derivative **4Ru**, the effect of  $\pi$ -backdonation was only noticed by the measurable negative shift of  $-20\text{ cm}^{-1}$  on the N $\equiv$ C stretching vibration since the <sup>1</sup>H NMR chemical shifts of the chromophore nitrile ligand remained unchanged after coordination. The effect of  $\pi$ -backdonation was already found in our previous studies involving monocyclopentadienyliron(II) and ruthenium(II) phosphine containing fragments possessing other chromophore ligands also coordinated by the nitrile functional group [7–10].

<sup>13</sup>C NMR data for this family of compounds confirm the evidence found for proton spectra. The Cp ring chemical shifts are in the range usually observed for Ru(II) and Fe(II) cationic derivatives, a significant deshielding ( up to  $\sim 14\text{ ppm}$ ) being observed on the carbon of the N $\equiv$ C functional group upon coordination, except for compound **4Ru** which chemical shift remained unchanged after coordination. All the other carbons of the chromophore ligand were only slightly deshielded or remained almost unchanged for the entire family of compounds.

<sup>31</sup>P{<sup>1</sup>H} NMR data of the complexes showed a single sharp signal for the phosphine coligands revealing an expected deshielding upon coordination, according to the  $\sigma$  donor character of these ligands.

### 2.3. UV-Vis studies

The optical absorption spectra of all complexes [M( $\eta^5$ -C<sub>5</sub>H<sub>5</sub>)(L<sub>2</sub>)(BDT)][PF<sub>6</sub>] were recorded in 10<sup>-4</sup> M dichloromethane and methanol solutions (Table 2) in order to identify the M  $\leftarrow$  L charge transfer and  $\pi$ - $\pi^*$  absorption bands expected for these complexes.

The electronic spectra of all the compounds showed two intense absorption bands in the UV region, attributed to electronic transitions occurring both in the organometallic fragment {MCp(LL)}<sup>+</sup> ( $\lambda \sim 235\text{ nm}$ ) and in the BDT coordinated chromophores ( $\lambda \sim 280$ – $340\text{ nm}$ ). Additionally, for the compounds containing DDPE as coligand, namely [Ru( $\eta^5$ -C<sub>5</sub>H<sub>5</sub>)(DPPE)(L1)][PF<sub>6</sub>] (**2Ru**), [Fe( $\eta^5$ -C<sub>5</sub>H<sub>5</sub>)(DPPE)(L1)][PF<sub>6</sub>] (**2Fe**) and [Fe( $\eta^5$ -C<sub>5</sub>H<sub>5</sub>)(DPPE)(L2)][PF<sub>6</sub>] (**3Fe**), evidence was found for the existence of charge transfer (CT) bands, appearing as shoulders on the intense absorption band

**Table 2**

Optical spectra data for complexes  $[M(\eta^5\text{-C}_5\text{H}_5)(\text{L}_\text{L})(\text{BDT})][\text{PF}_6]$ , **1Ru**, **2Ru**, **2Fe**, **3Fe**, **4Ru**, and the free **L1** and **L2** ligands, in dichloromethane and methanol (ca.  $10^{-4}$  M) solutions

Compound	$\lambda_{\text{max}}$ (nm) ( $\epsilon$ , $\text{M}^{-1} \text{cm}^{-1}$ )	
	$\text{CH}_2\text{Cl}_2$	MeOH
Benzo[1,2- <i>b</i> ;4,3- <i>b'</i> ]dithiophene ( <b>3</b> )	251 (12,500)	–
	289 (14,300)	–
	299 (sh)	–
Benzo[1,2- <i>b</i> ;4,3- <i>b'</i> ]-2-nitrodithiophene ( <b>5</b> )	264 (4800)	–
	285 (390)	–
	379 (7800)	–
	–	–
Benzo[1,2- <i>b</i> ;4,3- <i>b'</i> ]dithiophen-2-carbonitrile ( <b>L1</b> )	269 (12,600)	–
	276 (sh)	–
	315 (24,300)	–
$[\text{Ru}(\eta^5\text{-C}_5\text{H}_5)(\text{PPh}_3)_2(\text{L1})][\text{PF}_6]$ ( <b>1Ru</b> )	349 (23,800)	345 (23,400)
$[\text{Ru}(\eta^5\text{-C}_5\text{H}_5)(\text{PPh}_3)_2(\text{L1})][\text{CF}_3\text{SO}_3]$ ( <b>1'Ru</b> )	351 (23,500)	346 (22,900)
$[\text{Ru}(\eta^5\text{-C}_5\text{H}_5)(\text{dppe})(\text{L1})][\text{PF}_6]$ ( <b>2Ru</b> )	336 (19,000)	345 (22,400)
$[\text{Fe}(\eta^5\text{-C}_5\text{H}_5)(\text{dppe})(\text{L1})][\text{PF}_6]$ ( <b>2Fe</b> )	320 (13,200)	317 (11,200)
	347 (sh)	347 (sh)
	367 (sh)	363 (sh)
	423 (sh)	416 (sh)
	269 (11,700)	267 (11,700)
	315 (19,000)	313 (17,700)
$[\text{Ru}(\eta^5\text{-C}_5\text{H}_5)(\text{tmeda})(\text{L1})][\text{PF}_6]$ ( <b>4Ru</b> )	272 (6800)	–
	364 (6400)	–
	–	–
Benzo[1,2- <i>b</i> ;4,3- <i>b'</i> ]dithiophen-2'-nitro-2-carbonitrile ( <b>L2</b> )	361 (15,800)	355 (14,600)
	460 (sh)	460 (sh)

sh: shoulder.

of the **BDT** ligand, in the visible region of the spectra. The bathochromic shift observed for most of the bands when dichloromethane was substituted by methanol is compatible with the origin of these bands. Further studies in solvents of different polarities, to examine the solvatochromic effect, were limited by the low solubility of the compounds. Fig. 2 depicts the electronic spectra of the iron compounds **2Fe** and **3Fe**, together with the spectra of the related free **BDT** ligands, **L1** and **L2** for comparison.

For a better understanding of the electronic spectra of the studied compounds and the **L1** and **L2** uncoordinated ligands, additional studies were also carried out on the parent unsubstituted chromophore benzo[1,2-*b*;4,3-*b'*]dithiophene (**3**), and on the related compound benzo[1,2-*b*;4,3-*b'*]-2-nitrodithiophene (**5**) (see Scheme 1) to evaluate the effect of the substituting groups NC and NO<sub>2</sub> on the benzodithiophene parent molecule **3**. The compar-

ison of these electronic spectra is shown in Fig. 3. The effect of the introduction of one acceptor group on benzo[1,2-*b*;4,3-*b'*]dithiophene (**3**), either NC or NO<sub>2</sub>, leads to the expected bathochromic shift on the observed bands, as can be observed on the spectra of **L1** and compound **5**. Moreover, when both groups are competing in the same molecule, such as the case of **L2**, the stronger accepting effect of NO<sub>2</sub> is predominant as can be clearly observed by comparison of **L2** and **5**.

#### 2.4. X-ray structural studies of complexes **1Ru**, **1'Ru**, **2Ru** and **2Fe**

Compounds  $[\text{Ru}(\eta^5\text{-C}_5\text{H}_5)(\text{PPh}_3)_2(\text{NCC}_{10}\text{H}_5\text{S}_2)][\text{PF}_6] \cdot (\text{CH}_3)_2\text{CO}$  (**1Ru**) and  $[\text{Fe}(\eta^5\text{-C}_5\text{H}_5)(\text{DPPE})(\text{NCC}_{10}\text{H}_5\text{S}_2)][\text{PF}_6] \cdot (\text{CH}_3)_2\text{CO} \cdot \text{H}_2\text{O}$  (**2Fe**) were recrystallized by slow diffusion of *n*-heptane in acetone solutions and compound  $[\text{Ru}(\eta^5\text{-C}_5\text{H}_5)(\text{DPPE})(\text{NCC}_{10}\text{H}_5\text{S}_2)][\text{PF}_6]$  (**2Ru**) by slow diffusion of *n*-hexane in an acetone solution, affording suitable crystals for X-ray diffraction studies. Orange crystals of  $[\text{Ru}(\eta^5\text{-C}_5\text{H}_5)(\text{PPh}_3)_2(\text{NCC}_{10}\text{H}_5\text{S}_2)][\text{CF}_3\text{SO}_3] \cdot 0.5\text{CH}_2\text{Cl}_2$  (**1'Ru**) were obtained by slow diffusion of *n*-hexane in a dichloromethane solution. This compound was found to crystallize with two independent molecules in the asymmetric unit ( $Z' = 2$ ). Selected bond distances and angles are presented in Table 3, as well as the torsion angles.

The molecular structures of the cations **1Ru**<sup>+</sup>, **1'Ru**<sup>+</sup>, **2Ru**<sup>+</sup> and **2Fe**<sup>+</sup> are shown in Fig. 4–7.

All the complexes present the usual three-legged piano stool geometry around the metal atom, confirmed by the N–M–P angles, close to 90° (see Table 3) with the remaining C( $\eta^5$ -centroid)–M–X (with X = N or P) angles between 117.84(5)° and 130.6(6)°. Also, in all compounds, the benzodithiophene ligand is essentially planar with torsion angles between rings ranging from 175.0(5)° to 179.9(5)° (see Table 3).

All the Ru compounds show bond distances Ru–N as well the N–C placed in the range of the ones found for similar cyclopentadienyldiphosphine complexes with thiophene based nitriles ligands [29] (Ru–N 1.977–2.023 Å and N–C 1.139–1.178 Å) but smaller, in general, than the ones found in cyclopentadienyldiphosphine complexes with NPh ligands presented in Table 4. Although some results in this table, such as for example Ru–N distances, might suggest some evidence for  $\pi$ -backdonation on the compounds of the present study, compared to other related nitriles, a careful study of the other coordination geometrical param-

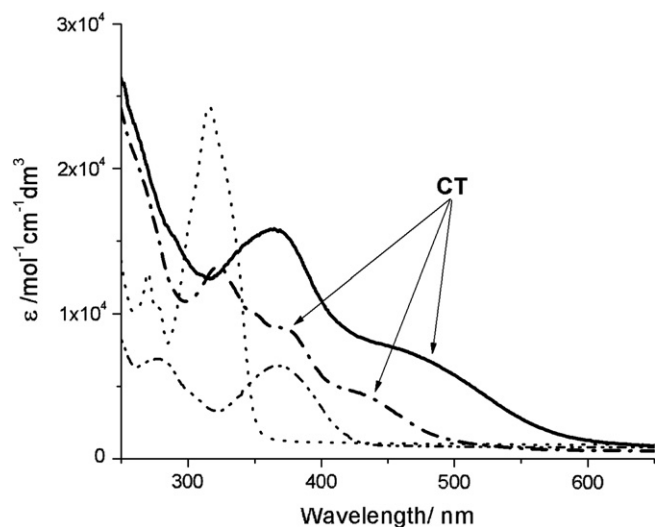


**Fig. 2.** Electronic spectra of  $[\text{Fe}(\eta^5\text{-C}_5\text{H}_5)(\text{DPPE})(\text{L1})][\text{PF}_6]$  **2Fe** (---), and  $[\text{Fe}(\eta^5\text{-C}_5\text{H}_5)(\text{DPPE})(\text{L2})][\text{PF}_6]$  **3Fe** (—), compared to the free ligands **L1** (cdots) and **L2** (— · —).

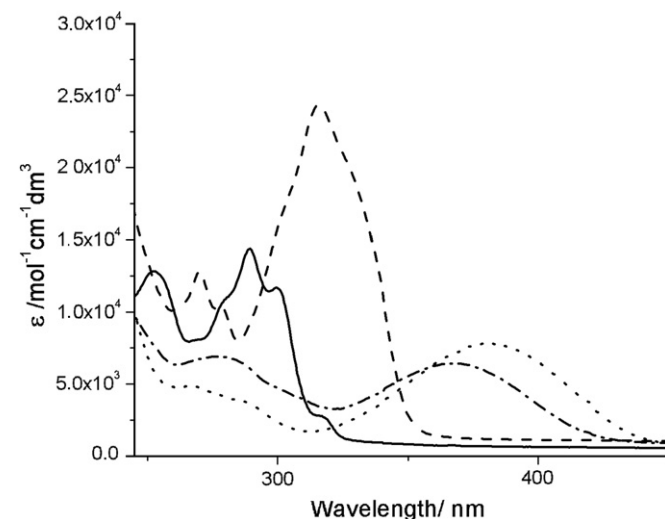


**Fig. 3.** Electronic spectra of free ligands **L1** (---) and **L2** (— · —), compared to the unsubstituted benzodithiophene, **3** (—), and nitrobenzodithiophene, **5** (···).

**Table 3**  
Selected bond lengths and bond and torsion angles for **1Ru**, **1'Ru**, **2Ru**, **2Fe**

Compound	<b>1Ru</b>	<b>1'Ru</b>	<b>2Ru</b>	<b>2Fe</b>
<i>Bond lengths (Å)</i>				
M–Cp	1.8539(12)	1.8590(5); 1.8648(6)	1.8639(4)	1.7132(7)
M–N(1)	1.995(6)	2.025(5); 2.016(6)	2.018(4)	1.8639(4)
N(1)–C(1)	1.117(10)	1.153(8); 1.151(9)	1.149(6)	1.154(6)
M(1)–P(1)	2.343(2)	2.3313(17); 2.3258(18)	2.2918(13)	2.2145(15)
M(1)–P(2)	2.352(2)	2.3600(17); 2.3334(18)	2.3041(12)	2.2088(15)
C(ar)–C(ar)	1.357–1.414	1.349–1.413	1.358–1.407	1.366–1.391
<i>Angles (°)</i>				
N(1)–M(1)–P(1)	91.27(18)	87.61(15); 88.76(16)	87.41(12)	92.66(13)
N(1)–M(1)–P(2)	87.82(19)	92.92(15); 94.90(17)	92.82(11)	84.73(13)
P(2)–M(1)–P(1)	104.83(7)	99.33(6); 100.57(6)	83.76(4)	86.83(6)
Cp–M(1)–N(1)	126.53(18)	126.55(14); 124.63(15)	124.64(11)	124.94(12)
Cp–M(1)–P(1)	117.84(5)	121.52(5); 119.98(5)	129.39(3)	124.48(5)
Cp–M(1)–P(2)	121.48(6)	120.75(4); 120.82(5)	126.03(4)	130.55(5)
M(1)–N(1)–C(1)	176.6(7)	176.3(5); 169.8(6)	176.7(4)	176.6(4)
N(1)–C(1)–C(2)	176.0(9)	173.4(7); 178.6(7)	176.3(6)	178.1(5)
<i>Torsion angles (°)</i>				
M(1)–N(1)–C(1)–C(2)	43(21)	–39(13); –127(34)	–116(9)	133(13)
N(1)–C(1)–C(2)–C(3)	–43(13)	–107(6); 164(35)	73(9)	–175(10)
N(1)–C(1)–C(2)–S(1)	137(12)	68(6); –16(36)	–103(9)	6(15)
C(1)–C(2)–C(3)–C(4)	177.8(7)	175.6(6); 176.6(7)	–175.0(5)	–177.7(4)
C(2)–C(3)–C(4)–C(9)	–176.9(9)	–179.9(6); –176.7(7)	176.6(5)	177.5(5)

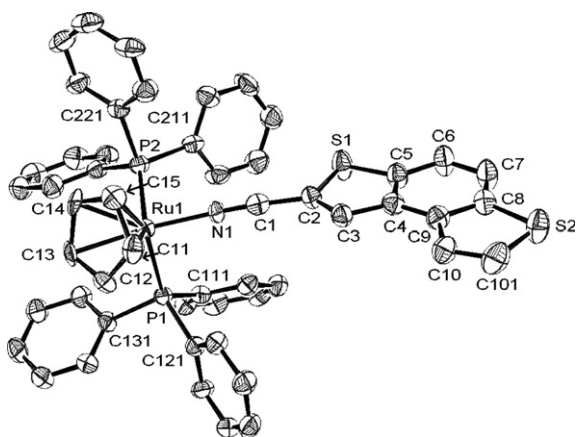


**Fig. 4.** ORTEP of the cation of compound  $\text{Ru}(\eta^5\text{-C}_5\text{H}_5)(\text{PPh}_3)_2(\text{L1})[\text{PF}_6] \cdot (\text{CH}_3)_2\text{CO}$ , **1Ru**.

eters do not lead us to any conclusion or evidence about the significance of this effect.

“Accordingly, also in complex **2Fe** the Fe–N and N–C bond lengths (1.8639(4) and 1.154(6) Å, respectively) are within the values found for complex  $[\text{CpFe}(\text{DPPE})(\text{NCSC}_4\text{H}_2\text{CH}=\text{CHSC}_4\text{H}_3)]^+[\text{PF}_6]^-$  (1.869(9) and 1.152(12) Å, respectively) [29] where also only spectroscopic evidence for back-donation was found”.

Detailed analysis of the geometric parameters in the four compounds, led us to notice that in compounds **2Ru** and **2Fe**, the **BDT** ligand is almost perpendicular with respect to the plane defined by the metal atom, the centroid of the cyclopentadienyl and the N1 and C1 atoms making a dihedral angle of 83.4(1)° and 86.5(1)°, respectively, while for **1Ru** the thiophene lies in a slightly twisted arrangement (dihedral angle 34.7(2)°). This, we thought, was due to the larger cone angle of the triphenylphosphine ligands (145°) in comparison with the cone angle of the diphenylphosphinoethane ligand (125°). However, in compound **1'Ru**, that has coordinated triphenylphosphine ligands, the two independent molecules in the unit cell, Fig. 8, are quite different: molecule labelled **A** the thiophene ligand has an arrangement similar to compounds **2Ru** and **2Fe**, i.e., the thiophene ligand is almost perpendicular with respect to the plane defined above, dihedral angle of 71.2(1)°, while the molecule labelled **B** has an arrangement analogous to the cation of compound **1Ru** where the **BDT** ligand is almost coplanar to this plane (dihedral angle 22.1(1)°). In a survey in CSD [34] of similar organometallic compounds with either Ru or Fe, PPh<sub>3</sub>, DPPE and nitriles or acetylides derivatives, no trend was observed. So the different arrangements can be attributed to an interplay of energetic stability and stereochemical hindrance. Analysing the stereochemical arrangements, the geometrical parameters to take in account should be the cone angle, the mono or bidentate behaviour of the phosphine, the size of the ligand and the supramolecular interactions in the crystal packing.

The different position of the **BDT** ligand in molecule **A** and **B** of **1'Ru** complex can be explained by the different supramolecular hydrogen bonding interactions between the CF<sub>3</sub>SO<sub>3</sub> anion and the ligand. In anion B only one of the oxygen atoms (O1B) interacts with two different hydrogens atoms, one from the adjacent carbon (C3B) of the **BDT** ligand and the other from the C15B carbon of the Cp ligand, forming a chelated hydrogen bond [35]. In the case of anion A these interactions are also established but through two different oxygen atoms of the triflate anion (O2A and O3A) with the hydrogen H3A of the **BDT** ligand and the H15A of the Cp ligand of cation A (see Table 5 and Fig. 8).

The crystal packing of **1Ru** discloses a very interesting supramolecular array, that displays holes in the *a* direction (Fig. 9), suggesting that this network can possibly be used as a selectively storing guests material [36,37]. This particular array is formed by intermolecular hydrogen bonds between one fluorine atom (F3) of the anion with the previously mentioned hydrogen atoms of the carbons of the **BDT** and carbon of the Cp, respectively H3 and H11, like in molecule A of the **1Ru** complex; but it is further extended, due to the interaction of the anion and the solvent molecule (F2···H20f–C202) and the short hydrogen bond of the oxygen of the solvent molecule with both H7 and H12, again from the **BDT** and Cp ligands of the cation, respectively (see Table 5). This supramolecular geometry implies that two cation molecules have no direct connection and their interactions are always mediated by the presence of the anion and solvent molecule, giving rise to the observed porosity, with holes of about 8 Å. This arrangement seems to be a result of the configuration of the **BDT** ligand towards the plane defined by the metal atom, the centroid of the cyclopentadienyl and the N1 and C1 atoms, as in molecule B of the compound **1Ru**.

As expected, the variation of the counter-ion in the cationic complex  $[\text{Ru}(\eta^5\text{-C}_5\text{H}_5)(\text{PPh}_3)_2(\text{NCC}_{10}\text{H}_5\text{S}_2)]^+$  from PF<sub>6</sub><sup>−</sup> to CF<sub>3</sub>SO<sub>3</sub><sup>−</sup> leads to very different arrays in the solid state, as can be seen on Fig. 9. While **1Ru** discloses a very interesting supramolecular arrangement, the crystal packing of the compound **1Ru** has a much more closed packing, due to the high number of hydrogen bonds of both anions present in the asymmetric unit. CF<sub>3</sub>SO<sub>3</sub><sup>−</sup> anion B has a bifurcated hydrogen bond with molecule B, as described above, while atom O2B interacts with a phenyl group of a symmetry related

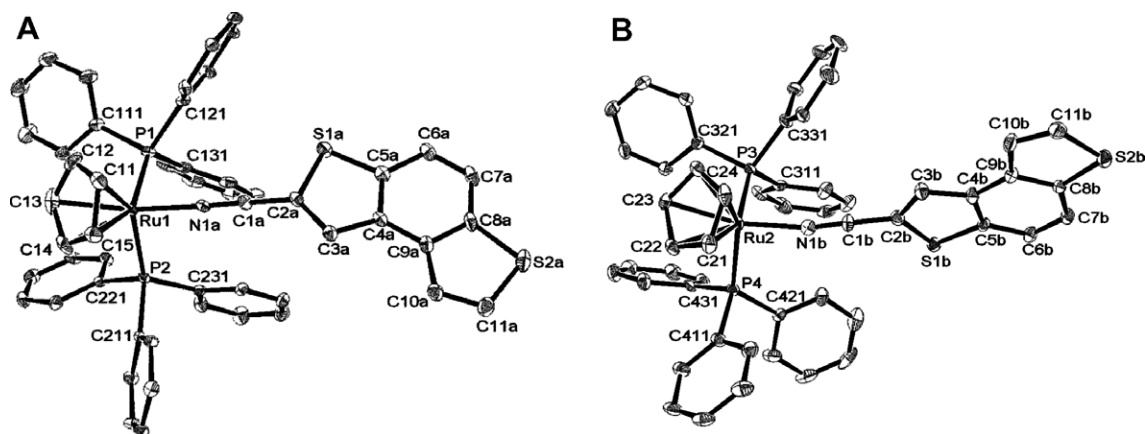


Fig. 5. ORTEP of the cation of compound  $\text{Ru}(\eta^5\text{-C}_5\text{H}_5)(\text{PPh}_3)_2(\text{L1})][\text{CF}_3\text{SO}_3] \cdot 0.5\text{CH}_2\text{Cl}_2$ , **1Ru**. The numbering **A** and **B** shows the two different independent molecules in the unit cell (see text).

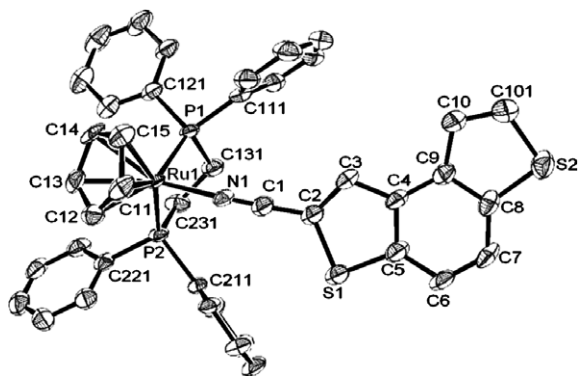


Fig. 6. ORTEP of the cation of compound  $[\text{Ru}(\eta^5\text{-C}_5\text{H}_5)(\text{dppe})(\text{L1})][\text{PF}_6]$ , **2Ru**.

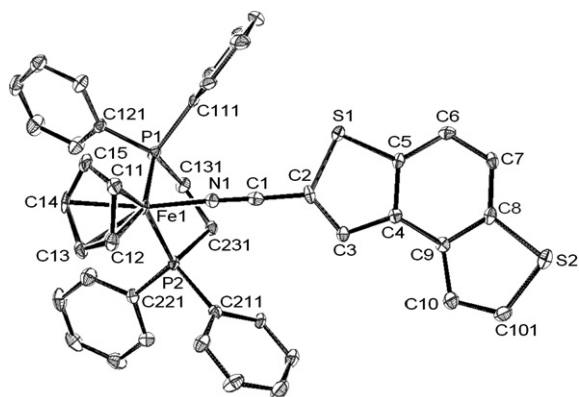


Fig. 7. ORTEP of the cation of compound  $\text{Fe}(\eta^5\text{-C}_5\text{H}_5)(\text{dppe})(\text{L1})][\text{PF}_6] \cdot (\text{CH}_3)_2\text{CO} \cdot \text{H}_2\text{O}$ , **2Fe**.

cation B and, moreover, a fluorine atom of the same anion still interacts with a phenyl group of another symmetry generated B molecule. At the same time, two of the oxygen atoms (O2A and O3A) of anion A interact with one A cation, while O1A interacts with another A cation. This complex tridimensional hydrogen bonds system explains the two diverse packings obtained. This is further complicated due to the presence of one dichloromethane molecule, which interacts with both cations at the same time.

Compound **2Ru** forms chains along the *a* direction due to the interaction of the  $\text{PF}_6$  molecule connecting two successive cations (see Table 5). This supramolecular packing is further enhanced

by a hydrogen bond between the external sulphur of the **BDT** ligand with an hydrogen of the ethylene fragment of the phosphine, leading to the formation of a pseudo-dimeric motif (Fig. 10).

The analysis of the crystalline structure of compound **2Fe** reveals that it also forms pseudo-dimeric units, *via* intermolecular interactions with the  $\text{PF}_6$ , almost bisecting the *ab* plane. These dimers are reinforced through  $\pi$ - $\pi$  interactions of the **BDT** ligand (Fig. 11).

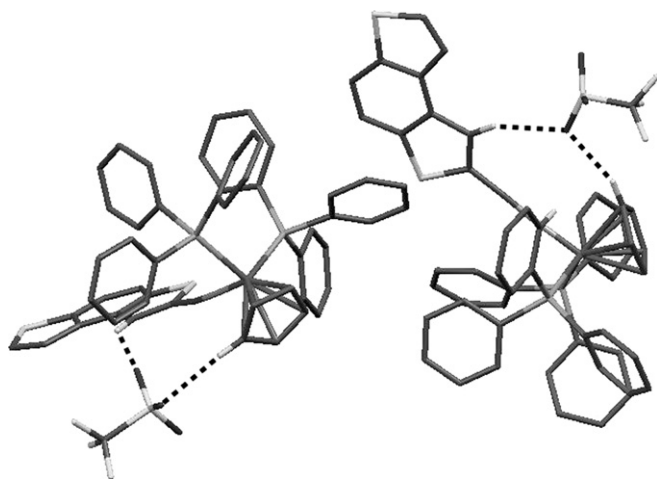
### 2.5. Electrochemical studies

In order to obtain an insight on the electron richness of the organometallic fragment and on the coordinated **BDT** ligands, the electrochemical behaviour of Ru(II) and Fe(II) compounds and also the free **BDT** chromophores **L1** and **L2**, were studied by cyclic voltammetry in dichloromethane and acetonitrile, between the limits imposed by the solvents. Similar studies were also carried out on the related molecules benzo[1,2-*b*;4,3-*b'*]dithiophene (**3**) and benzo[1,2-*b*;4,3-*b'*]-2'-nitrodithiophene (**5**) (see Scheme 1) for a better understanding on the behaviour of the ligands **L1** and **L2**. Tables 6 and 7 summarize the electrochemical data obtained for all the studied compounds in dichloromethane and acetonitrile, respectively, at room temperature and at the scan rate of  $200 \text{ mV s}^{-1}$ . Studies carried out at scan rates of 50 and  $100 \text{ mV s}^{-1}$  showed the same results. The electrochemistry of the free ligand **L1** was characterized by an irreversible oxidation at  $E_{\text{pa}}$  value of +1.48 V in dichloromethane and no reductive processes were found at negative potentials. The behaviour of **L1** in acetonitrile was quite different, since besides the oxidation process occurring at  $E_{\text{pa}} = +1.38 \text{ V}$ , with a very weak counterpart at  $E_{\text{pc}} = +1.28 \text{ V}$ , one reductive process was also observed presenting a cathodic wave at  $E_{\text{pc}} = -1.70 \text{ V}$  with a very small counterpart at  $E_{\text{pa}} = -1.56 \text{ V}$ . The related compound **3** presented only one anodic process occurring in both solvents at a somehow higher potential than **L1**,  $E_{\text{pa}} = +1.55 \text{ V}$  ( $\text{CH}_2\text{Cl}_2$ ) and  $E_{\text{pa}} = +1.45 \text{ V}$  ( $\text{CH}_3\text{CN}$ ). For this compound, no reductive processes were observed. The cyclic voltamogram of the ligand **L2**, shows clearly the influence of the good acceptor  $\text{NO}_2$  group, presenting two irreversible redox processes at  $E_{\text{pc}} = -0.88$  ( $E_{\text{pa}} = -0.76 \text{ V}$ ) and  $E_{\text{pc}} = -1.29$  ( $E_{\text{pa}} = -1.17 \text{ V}$ ) in dichloromethane, and also one additional cathodic wave at  $E_{\text{pc}} = -1.50 \text{ V}$ . In acetonitrile the three processes were also observed at lower potentials, displaying two irreversible processes at  $E_{\text{pc}} = -0.85$  ( $E_{\text{pa}} = -0.77 \text{ V}$ ) and  $E_{\text{pc}} = -1.26$  ( $E_{\text{pa}} = -1.14 \text{ V}$ ). In this solvent, the third reducing process at  $E_{\text{pc}} = -1.57 \text{ V}$  showed a small anodic counterpart at  $E_{\text{pa}} = -1.43 \text{ V}$ . As would be expected, the related molecule **5** shows also two irreversible redox processes

**Table 4**

Comparison the geometrical parameters for ruthenium and iron derivatives containing MCp(phosphine) nitrile cations and the ones presented in this work

Compound	M–N (Å)	N–C (Å)	C–C (Å)	M–N–C (°)	N–C–C (°)	Ref.
[RuCp(PPh <sub>3</sub> ) <sub>2</sub> (NCPh)][PF <sub>6</sub> ]	2.037(1)	1.145(2)	1.440(2)	171.70(12)	177.84(16)	[30]
[RuCp(PPh <sub>3</sub> ) <sub>2</sub> (NCPhNO <sub>2</sub> )] [PF <sub>6</sub> ]	2.023(2)	1.146(2)	1.442(3)	171.24(15)	177.8(2)	[30]
[RuCp((+)-DIOP)(NCPhNO <sub>2</sub> )] [PF <sub>6</sub> ]	2.031(13)	1.137(18)	1.42(2)	177.2(12)	178.6(15)	[14]
[RuCp(PPh <sub>3</sub> ) <sub>2</sub> (NCPhNMe <sub>2</sub> )] [PF <sub>6</sub> ]	2.031(1)	1.149(2)	1.424(2)	173.52(14)	175.15(18)	[30]
[RuCp(PPh <sub>3</sub> ) <sub>2</sub> (NCPh)] [PF <sub>6</sub> ]	2.037(1)	1.145(2)	1.440(2)	171.7(1)	177.8(2)	[31]
[RuCp(PPh <sub>3</sub> ) <sub>2</sub> (L1)] [PF <sub>6</sub> ] · (CH <sub>3</sub> ) <sub>2</sub> CO	1.995(6)	1.117(10)	1.464(12)	176.6(7)	176.0(9)	– <sup>a</sup>
[RuCp(PPh <sub>3</sub> ) <sub>2</sub> (L1)] [CF <sub>3</sub> SO <sub>3</sub> ] · 0.5CH <sub>2</sub> Cl <sub>2</sub>	2.025(5); 2.016(6)	1.153(8); 1.151(9)	1.402(9); 1.416(10)	176.3(5); 169.8(6)	173.4(7); 178.6(7)	– <sup>a</sup>
[RuCp(DPPE)(L1)] [PF <sub>6</sub> ]	2.018(4)	1.149(6)	1.400(7)	176.7(4)	176.3(6)	– <sup>a</sup>
[FeCp(DPPE)(NCPh)] [PF <sub>6</sub> ]	1.892(2)	1.141(3)	1.444(3)	172.16(18)	174.5(2)	[30]
[FeCp(DPPE)(NCPhNO <sub>2</sub> )] [PF <sub>6</sub> ]	1.874(11)	1.129(14)	1.42(2)	176.6(11)	177.4(15)	[9]
[FeCp(DPPE)(NCPhNO <sub>2</sub> )] [1]	1.875(13)	1.390(19)	1.40(2)	175.6(11)	178.0(16)	[32]
[FeCp(PROPHOS)(NCPhNO <sub>2</sub> )] [PF <sub>6</sub> ]	1.902(9)	1.142(15)	1.421(15)	172.0(10)	172.8(13)	[33]
[FeCp(DPPE)(L1)] [PF <sub>6</sub> ] · (CH <sub>3</sub> ) <sub>2</sub> CO · H <sub>2</sub> O	1.8639(4)	1.154(6)	1.427(8)	176.6(4)	178.1(5)	– <sup>a</sup>

<sup>a</sup> This work; DPPE = 1,2-bis(diphenylphosphino)ethane; PROPHOS = (R)-(+)-1,2-Bis(diphenylphosphino)- propane.**Fig. 8.** Supramolecular interactions responsible for the different positioning of the BDT ligand towards the plane defined by the metal atom, the centroid of the cyclopentadienyl and the N1 and C1 atoms, in the two molecules of the unit cell of **1Ru** complex.**Table 5**Intermolecular contacts [Å] for compounds **1Ru**, **1Ru**, **2Ru**, **2Fe**

<b>1Ru</b>		<b>1Ru</b>	
C3–H3...F3	2.522(9)	C3A–H3A...O2A	2.531(7)
C3–H3...F2	2.588(13)	C15A–H15A...O3A	2.551(6)
C11–H11...F3	2.577(11)	C3B–H3B...O1B	2.416(9)
C7–H7...O1	2.491(8)	C15B–H15B...O1B	2.453(8)
C12–H12...O1	2.459(10)		
<b>2Ru</b>		<b>2Fe</b>	
C13–H13A...S2	2.917(2)	C5...C9	3.383(12)
C223–H223...F5	2.643(5)	C10–H10...F5	2.588(4)
C224–H224...F3	2.435(5)	C6–H6...F2	2.561(3)
C226–H226...F4	2.620(5)	C213–H213...F2	2.470(3)
C216–H216...F4	2.571(4)		
C216–H216...F5	2.654(6)		
C12–H12...F4	2.584(5)		

at  $E_{pc} = -0.98$  V ( $E_{pa} = -0.83$  V), in dichloromethane, revealing the presence of NO<sub>2</sub>. These processes occurred in acetonitrile at  $E_{pc} = -0.94$  V ( $E_{pa} = -0.80$  V) and  $E_{pc} = -1.04$  V ( $E_{pa} = -0.95$  V). Therefore, it seems that the reduction of compound **L2** is clearly easier than the reduction of the related molecules **L1**, **3** and **5**. These data, suggesting that this compound can potentially act as a good electron acceptor ligand, are in good agreement with the

found spectroscopic data, in particular the <sup>1</sup>H NMR experimental results discussed before for compound **3Fe**.

The general behaviour of the ruthenium compounds in both solvents was characterised by one oxidation process Ru<sup>II</sup>/Ru<sup>III</sup>, with  $E_{pa}$  in the range 1.10–1.40 V with a very small cathodic counterpart, while the iron analogues show a non reversible Fe<sup>II</sup>/Fe<sup>III</sup> redox process, with  $E_{p/2}$  placed in the range 0.70–0.90 V. For all the studied compounds, the electrochemical processes were easier in acetonitrile, as expected. Comparison of the values presented on Tables 6 and 7 for compounds possessing the coordinated BDT ligand **L1**, namely **1Ru**, **2Ru** and **2Fe** with the ones of the free compound **L1**, reveals some differences. In fact, as mentioned above, although no reductive processes were observed for **L1** in CH<sub>2</sub>Cl<sub>2</sub>, its electrochemical behaviour in CH<sub>3</sub>CN was more complex, showing a reductive process at  $E_{pc} = -1.70$  V with the corresponding anodic wave at  $E_{pa} = -1.56$  V. After coordination, this reductive process attributed to ligand **L1** occurs at less negative potentials for all the complexes possessing this ligand at  $E_{pc} = -1.53$  V for **1Ru**,  $E_{pc} = -1.61$  V for **2Ru**, and  $E_{pc} = -1.55$  V for **2Fe**, revealing the easier reducing ability of the coordinated ligand **L1**.

Regardless all the spectroscopic data for compound **2Fe** point out for some evidence of  $\pi$ -backbonding, corroborated by the X-ray data (Fe–N shorter distance than usual and the NC distance compatible with a double bond), the electrochemical behaviour of this compound is similar to the ruthenium related ones.

The electrochemical behaviour of compounds **3Fe** and free ligand **L2**, in dichloromethane, is illustrated in Fig. 12. Comparison of the electrochemistry of compounds **2Fe** and **3Fe** shows that compound **3Fe** oxidizes ~25 mV at higher potential than **2Fe**, in both solvents, suggesting that the metal centre is more deficient in electronic density. Accordingly, in compound **3Fe** the reduction on the coordinated ligand **L2** became more difficult, showing only one reductive process that occurs at  $E_{pc} = -0.90$  V (CH<sub>2</sub>Cl<sub>2</sub>) instead the three reductive processes observed for free **L2** ( $E_{pc} = -0.88$ ;  $-1.29$  and  $-1.50$  V) in the same solvent. These results can be related to an easier electronic flow from the metal centre, through the ligand, towards the nitro group, this being in good agreement with the <sup>1</sup>H and <sup>13</sup>C NMR, FT-IR and UV-Vis spectroscopic data, which suggest an increase of  $\pi$ -backdonation on compound **3Fe** when compared with **2Fe**.

## 2.6. Second harmonic generation (SHG)

In order to study the second harmonic generation, the complexes **2Ru**, **2Fe** and **3Fe** were subjected to hyper-Rayleigh scattering (HRS) studies [38]. To avoid the effect of fluorescence due to two-photon absorption and to obtain as little resonance

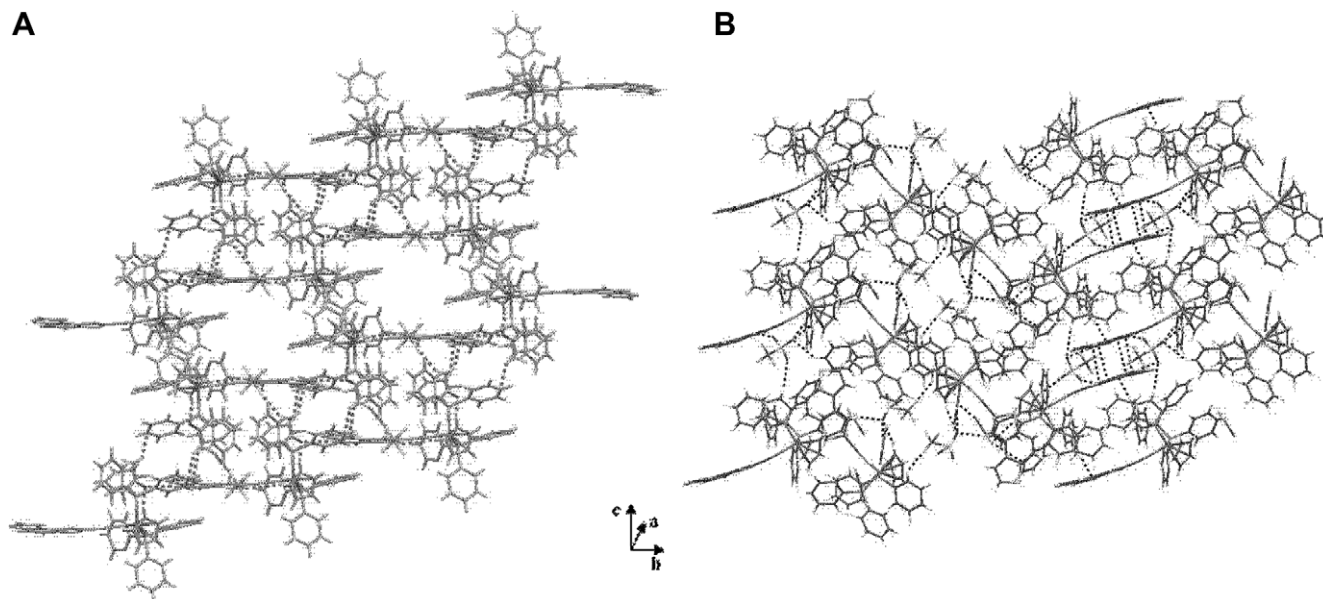


**Fig. 9.** Comparison of crystal packing in compounds containing the cationic complexes  $[\text{Ru}(\eta^5\text{-C}_5\text{H}_5)(\text{PPh}_3)_2(\text{L1})]^+$ : (A) Supramolecular array of compound with  $[\text{PF}_6]^-$  (**1Ru**), displaying holes in the *a* direction; (B) Crystal packing of compound with  $[\text{CF}_3\text{SO}_3]^-$  (**1'Ru**) along the *a* axis, showing the closer packing of the compound.

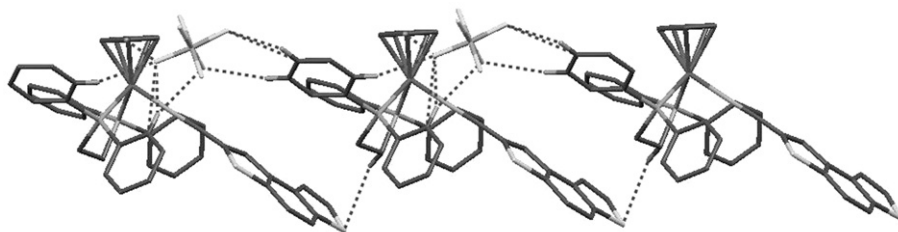


**Fig. 10.** Perspective view of the pseudo-dimeric motif of compound  $[\text{Ru}(\eta^5\text{-C}_5\text{H}_5)(\text{DPPE})(\text{L1})][\text{PF}_6]$ , **2Ru**, forming chains along the *a* direction.

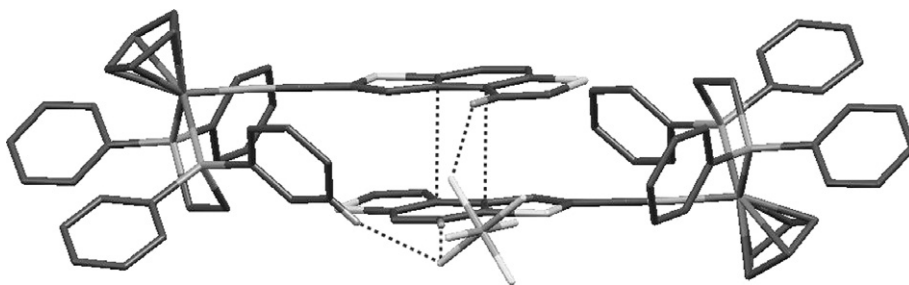


**Fig. 11.** Dimeric units of compound  $[\text{Fe}(\eta^5\text{-C}_5\text{H}_5)(\text{PPh}_3)_2(\text{L1})][\text{PF}_6]$ , **2Fe**, showing intermolecular  $\pi$ - $\pi$  interactions of the thiophene ligands.

enhancement as possible [39], the stimulating laser light was shifted from the original wavelength of the used Nd:YAG laser of 1064 nm to a higher wavelength (1500 nm). Thus, a superposition of absorptions in the UV-Vis region and the SHG signal (750 nm) is reduced, which makes the calculated static hyperpolarisability ( $\beta_0$ ) [39] more reliable [40,41]. Another important reason for using the higher wavelength incident beam, is an attempt to discriminate between a true SHG signal and a two photons absorption induced fluorescence (TPAF) enhanced signal [42,43]. The 1500 nm incident beam HRS examinations were achieved using a tuneable optical parametric oscillator (OPO) based set-up [41]. All measurements were carried out using Disperse Red 1 (DR1) as an external standard. The reference hyperpolarisability  $\beta$  of DR1 in  $\text{CH}_2\text{Cl}_2$  was calculated by comparison of the slopes of the standard in  $\text{CH}_2\text{Cl}_2$  and

$\text{CHCl}_3$ , to obtain the ratio of  $\beta_{\text{solute}}$  [44]. Using the value  $\beta(\text{CHCl}_3) = 80 \times 10^{-30}$  esu [45] the hyperpolarisability of DR1 in  $\text{CH}_2\text{Cl}_2$  is estimated to be  $70 \times 10^{-30}$  esu. The effect of the refractive indices of the solvents was corrected using the simple Lorentz local field [42]. Unfortunately, no SHG intensity could be detected for **2Ru** and **2Fe**, although the concentration of the investigated solutions of **2Fe** and **2Ru** were considerably high for this method ( $>10^{-3}$  M). However, the HRS study of **3Fe** results in a measurable, although weak SHG value. The calculated first hyperpolarizability amounts to  $\beta = 33 \times 10^{-30}$  esu. The corresponding static first hyperpolarizability is calculated to  $\beta_0 = 19 \times 10^{-30}$  esu taking into account the long wavelength absorption which is assigned to a donor-acceptor charge-transfer transition. The failure of a measurable SHG for **2Fe** and **2Ru** can be explained by the weak

**Table 6**

Electrochemical data for the complexes  $[M(\eta^5\text{-C}_5\text{H}_5)(\text{LL})(\text{BDT})][\text{PF}_6]$ , the free **BDT** ligands and the related compounds **3** and **5**, in  $\text{CH}_2\text{Cl}_2$

Compound	$E_{\text{pa}}$ (V)	$E_{\text{pc}}$ (V)	$E_{\text{p}1/2}$ (V)	$E_{\text{pa}} - E_{\text{pc}}$ (mV)	$I_{\text{a}}/I_{\text{c}}$
Benzo[1,2- <i>b</i> ;4,3- <i>b'</i> ]dithiophene ( <b>3</b> )	1.55	–	–	–	–
	–	–0.16 <sup>a</sup>	–	–	–
Benzo[1,2- <i>b</i> ;4,3- <i>b'</i> ]-2-nitrodithiophene ( <b>5</b> )	–0.83	–0.98	–0.91	150	–
	–0.98	–1.08	–1.02	100	–
Benzo[1,2- <i>b</i> ;4,3- <i>b'</i> ]dithiophen-2-carbonitrile ( <b>L3</b> )	1.48	–	–	–	–
$[\text{Ru}(\eta^5\text{-C}_5\text{H}_5)(\text{PPh}_3)_2(\text{L1})][\text{PF}_6]$ ( <b>1Ru</b> )	1.37	1.23	1.30	140	–
$[\text{Ru}(\eta^5\text{-C}_5\text{H}_5)(\text{DPPE})(\text{L1})][\text{PF}_6]$ ( <b>2Ru</b> )	1.53	–	–	–	–
	1.28	1.16	1.22	120	–
$[\text{Fe}(\eta^5\text{-C}_5\text{H}_5)(\text{DPPE})(\text{L1})][\text{PF}_6]$ ( <b>2Fe</b> )	0.89	0.81	0.85	80	≈1
Benzo[1,2- <i>b</i> ;4,3- <i>b'</i> ]dithiophen-2'-nitro-2-carbonitrile ( <b>L2</b> )	–0.76	–0.88	–0.82	120	–
	–1.17	–1.29	–1.23	120	0.9
	–	–1.50	–	–	–
$[\text{Fe}(\eta^5\text{-C}_5\text{H}_5)(\text{DPPE})(\text{L2})][\text{PF}_6]$ ( <b>3Fe</b> )	0.92	0.82	0.87	100	≈1
	–0.74	–0.90	–	–	–

<sup>a</sup> Small wave due to products originated by oxidation at 1.55 V.

**Table 7**

Electrochemical data for the complexes  $[M(\eta^5\text{-C}_5\text{H}_5)(\text{LL})(\text{BDT})][\text{PF}_6]$ , the free **BDT** ligands and the related compounds **3** and **5**, in  $\text{CH}_3\text{CN}$

Compound	$E_{\text{pa}}$ (V)	$E_{\text{pc}}$ (V)	$E_{\text{p}1/2}$ (V)	$E_{\text{pa}} - E_{\text{pc}}$ (mV)	$I_{\text{a}}/I_{\text{c}}$
Benzo[1,2- <i>b</i> ;4,3- <i>b'</i> ]dithiophene ( <b>3</b> )	1.45	–	–	–	–
	–	–0.02 <sup>a</sup>	–	–	–
Benzo[1,2- <i>b</i> ;4,3- <i>b'</i> ]-2-nitrodithiophene ( <b>5</b> )	–0.80	–0.94	–0.87	140	–
	–0.95	–1.04	–1.00	90	–
Benzo[1,2- <i>b</i> ;4,3- <i>b'</i> ]dithiophen-2-carbonitrile ( <b>L1</b> )	1.38	1.28	1.33	100	–
	–1.56	–1.70	–1.63	140	–
$[\text{Ru}(\eta^5\text{-C}_5\text{H}_5)(\text{PPh}_3)_2(\text{L1})][\text{PF}_6]$ ( <b>1Ru</b> )	1.38	–	–	–	–
	1.13	1.01	1.07	120	–
	–	–1.53	–	–	–
	–	–1.70	–	–	–
$[\text{Ru}(\eta^5\text{-C}_5\text{H}_5)(\text{DPPE})(\text{L1})][\text{PF}_6]$ ( <b>2Ru</b> )	1.11	1.01	1.06	100	–
	–	–1.61	–	–	–
$[\text{Fe}(\eta^5\text{-C}_5\text{H}_5)(\text{DPPE})(\text{L1})][\text{PF}_6]$ ( <b>2Fe</b> )	0.79	0.65	0.72	140	1.25
	–	–1.55	–	–	–
Benzo[1,2- <i>b</i> ;4,3- <i>b'</i> ]dithiophen-2'-nitro-2-carbonitrile ( <b>L2</b> )	–0.77	–0.85	–0.81	80	0.8
	–1.14	–1.26	–1.20	90	≈1
	–1.43	–1.57	–1.50	140	–
$[\text{Fe}(\eta^5\text{-C}_5\text{H}_5)(\text{DPPE})(\text{L2})][\text{PF}_6]$ ( <b>3Fe</b> )	0.81	0.64	0.73	–	≈1
	–0.73	–0.86	–0.79	130	–
	–	–1.40	–	–	–
	–	–1.63	–	–	–

<sup>a</sup> Small wave due to products originated by oxidation at 1.45 V.

$\pi$ -backbonding effect which barely compensates the ligand sigma coordination, as suggested by the spectroscopic and electrochemical data. The rather high energy shifted electronic excitation of **2Fe** and **2Ru** compared to **3Fe** which bares an electron accepting function ( $\text{NO}_2$ ), and the measurable SHG for **3Fe** confirm this interpretation.

### 3. Conclusion/summary

With the aim to continue the exploitation of the NLO properties originated by charge transfer metal-ligand through the interaction of  $d_{\pi^*}\pi_{\text{NC}}$  orbitals, a new family of Ru(II) and Fe(II) piano stool structured was synthesised and fully characterized. The main structural feature of these compounds is the planarity of the new chromophore coligands **BDT** guaranteed by the fused rings skeleton, with one phenyl ring placed between two thiophene units. Spectroscopic evidence by  $^1\text{H}$  NMR, UV–Vis, FT-IR and electrochemical studies by cyclic voltammetry, suggested some existence of a weak electronic delocalization due to the  $\pi$ -backbonding effect, on the iron derivatives **2Fe** and **3Fe**. Our preliminary evaluation on the quadratic hyperpolarizability

determined by hyper-Rayleigh scattering (HRS) at 1500 nm, found for **3Fe** the value of  $\beta_0 = 19 \times 10^{-30}$  esu, while for compounds **2Fe** (and also **2Ru**) the SHG values was negligible. In spite of, all the experimental data for compound **3Fe** point out for the existence of a donor-acceptor combination originated by the presence of the  $\text{NO}_2$  group, the value of SHG found was disappointingly small.

The crystallization of these compounds in centrosymmetric space groups precludes the evaluation of the NLO properties in the solid state by Kurtz powder technique.

## 4. Experimental

### 4.1. General procedures

All the experiments were carried out under dinitrogen atmosphere using standard Schlenk techniques. All the solvents used were dried using standard methods [46]. Starting materials  $[M(\eta^5\text{-C}_5\text{H}_5)(\text{LL})\text{X}]$  (LL = TMEDA, DPPE, 2PPh<sub>3</sub> and X = Cl when M = Ru, LL = DPPE and X = I when M = Fe) were prepared following the methods described in the literature [(i)  $[\text{Ru}(\eta^5\text{-C}_5\text{H}_5)(\text{DPPE})\text{Cl}]$  and  $[\text{Ru}(\eta^5\text{-C}_5\text{H}_5)(\text{PPh}_3)_2\text{Cl}]$  [47], (ii)  $[\text{Fe}(\eta^5\text{-C}_5\text{H}_5)(\text{DPPE})\text{I}]$  [9];  $[\text{Ru}(\eta^5\text{-C}_5\text{H}_5)(\text{TMEDA})\text{Cl}]$  [48]; Benzo[1,2-*b*;4,3-*b'*]dithiophen-2-carbaldehyde [28]. FT-IR spectra were recorded in a Mattson Satellite FT-IR spectrophotometer with KBr pellets; only significant bands are cited in text.  $^1\text{H}$ - $^{13}\text{C}$ - and  $^{31}\text{P}$  NMR spectra were recorded on a Bruker Avance 400 spectrometer at probe temperature. The  $^1\text{H}$  (DMSO-*d*<sub>6</sub>) and  $^{13}\text{C}$  (DMSO-*d*<sub>6</sub>) chemical shifts are reported in parts per million (ppm) downfield from internal Me<sub>4</sub>Si and the  $^{31}\text{P}$  (DMSO-*d*<sub>6</sub>) NMR spectra are reported in ppm downfield from external standard, 85% H<sub>3</sub>PO<sub>4</sub>. Elemental analyses were obtained at Laboratório de Análises, Instituto Superior Técnico, using a Fisons Instruments EA1108 system. Data acquisition, integration and handling were performed using a PC with the software package EAGER-200 (Carlo Erba Instruments). Melting points were obtained on a Reichert Thermovar equipment.

Electronic spectra were recorded at room temperature on a Jasco V-560 spectrometer in the range of 200–900 nm.

### 4.2. Synthesis of the hemi-helicene chromophore ligands

#### 4.2.1. Benzo[1,2-*b*;4,3-*b'*]dithiophen-2-carbonitrile (**L1**)

A solution of  $\text{H}_2\text{NOH} \cdot \text{HCl}$  (0.14 g, 2 mmol) in pyridine (4 mL) was added to a solution of benzo[1,2-*b*;4,3-*b'*]dithiophene (0.19 g, 1 mmol) in pyridine (4 mL) cooled to  $-30^\circ\text{C}$ . After stirring for 1 h at that temperature, acetic anhydride (5 mL) was added and the mixture was refluxed for 1 h. After cooling the mixture at room temperature, it was poured on cold water, the precipitate filtered and dissolved in methylene chloride (30 mL). The solution was washed with water ( $3 \times 20$  mL), the solvent removed under reduced pressure and the product purified by means of flash column chromatography (eluent: light petroleum/methylene chloride 7:3), affording 0.18 g (0.84 mmol, yield 84%) of pure benzo[1,2-*b*;4,3-*b'*]dithiophen-2-carbonitrile; m.p. 122–124°C. IR (KBr,  $\text{cm}^{-1}$ ):  $\nu(\text{CN})$  2215.  $^1\text{H}$  NMR (DMSO-*d*<sub>6</sub>): 8.05(d, 2H, H<sub>10</sub>, H<sub>11</sub>), 8.09(d, 1H, H<sub>7</sub>,  $J = 8.8$  Hz), 8.25(d, 1H, H<sub>6</sub>,  $J = 8.8$  Hz), 8.93(s, 1H, H<sub>3</sub>).  $^{13}\text{C}$  NMR (DMSO-*d*<sub>6</sub>): 107.85(C<sub>2</sub>), 114.74(CN), 118.43(C<sub>7</sub>), 122.40(C<sub>10</sub>), 123.02(C<sub>6</sub>), 129.57(C<sub>11</sub>), 132.45(C<sub>9</sub>), 134.70(C<sub>3</sub>), 135.00(C<sub>4</sub>), 136.99(C<sub>8</sub>), 138.50(C<sub>5</sub>). Anal. Calc. for C<sub>11</sub>H<sub>5</sub>NS<sub>2</sub>: C, 61.37; H, 2.34; N, 6.51; S, 29.78. Found: C, 61.20; H, 2.06; N, 5.91; S, 30.94%.

#### 4.2.2. Benzo[1,2-*b*;4,3-*b'*]dithiophen-2'-nitro-2-carbonitrile (**L2**)

Nitric acid (0.08 mL) was added to a solution of benzo[1,2-*b*;4,3-*b'*]dithiophen-2-carbonitrile (0.22 g, 1 mmol) in acetic anhydride (4 mL) at room temperature. After 1 h in agitation, the mixture was poured onto water, extracted with methylene chloride, washed

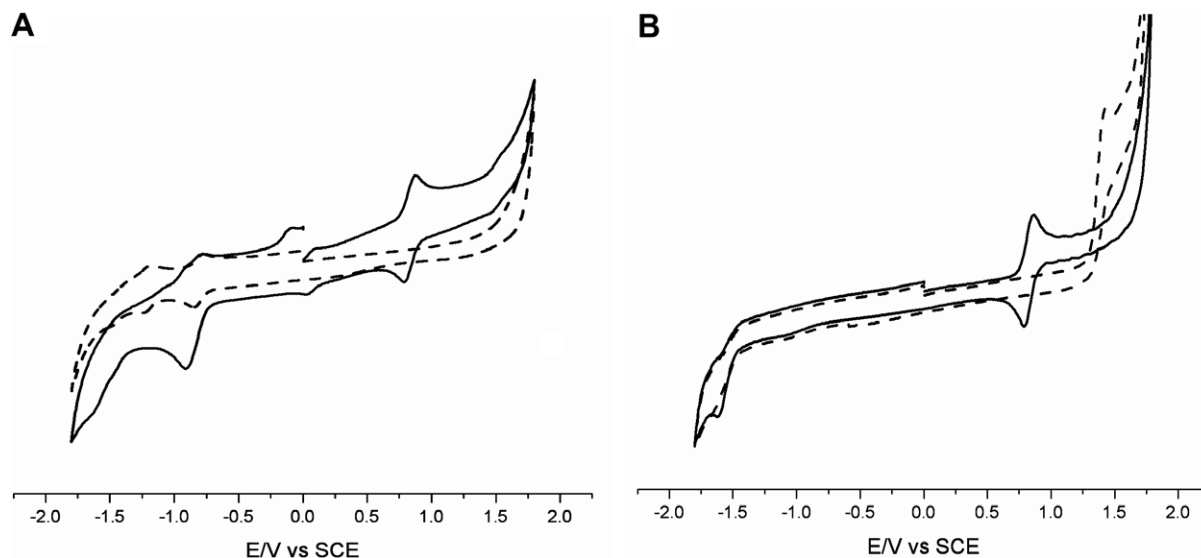


**Fig. 12.** Cyclic voltammograms in dichloromethane, at scan rate of  $200 \text{ mV s}^{-1}$ : (A)  $[\text{Fe}(\eta^5\text{-C}_5\text{H}_5)(\text{DPPE})(\text{L2})][\text{PF}_6]$ , **3Fe** (—), and the free ligand **L2** (---); (B)  $[\text{Fe}(\eta^5\text{-C}_5\text{H}_5)(\text{DPPE})(\text{L1})][\text{PF}_6]$ , **2Fe** (—), and the free ligand **L1** (---).

with saturated solution of  $\text{NaHCO}_3$  and water, dried with magnesium sulphate and the solvent removed. Recrystallization from methylene chloride/heptane afforded 0.12 g (0.46 mmol, yield 46%) of pure benzo[1,2-*b*;4,3-*b'*]dithiophen-2'-nitro-2-carbonitrile; m.p.  $130\text{--}131^\circ\text{C}$ . IR (KBr,  $\text{cm}^{-1}$ ):  $\nu(\text{CN})$  2216.  $^1\text{H}$  NMR (DMSO- $d_6$ ): 8.26(d, 1H,  $\text{H}_6$ ,  $J = 9.0 \text{ Hz}$ ), 8.35(d, 1H,  $\text{H}_7$ ,  $J = 9.0 \text{ Hz}$ ), 8.95(s, 1H,  $\text{H}_3$ ), 9.08(s, 1H,  $\text{H}_{10}$ ).  $^{13}\text{C}$  NMR (DMSO- $d_6$ ): 110.50( $\text{C}_2$ ), 114.86( $\text{C}\equiv\text{N}$ ), 123.42( $\text{C}_6$ ), 124.57( $\text{C}_7$ ), 125.51( $\text{C}_{10}$ ), 132.18( $\text{C}_5$ ), 134.58( $\text{C}_8$ ), 135.00( $\text{C}_3$ ), 139.06( $\text{C}_4$ ), 140.34( $\text{C}_9$ ), 151.97( $\text{C}_{11}$ ). Anal. Calc. for  $\text{C}_{11}\text{H}_5\text{NS}_2$ : C, 50.76; H, 1.55; N, 10.76; S, 24.63. Found: C, 50.91; H, 1.34; N, 10.69; S, 24.48%.

#### 4.2.3. Benzo[1,2-*b*;4,3-*b'*] -2'-nitrodithiophene (**5**)

Nitric acid (0.08 mL) was added to a solution of benzo[1,2-*b*;4,3-*b'*]dithiophene (0.19 g, 1 mmol) in acetic anhydride (4 mL)  $5^\circ\text{C}$ . After 1 h with stirring, the mixture was poured on to water, extracted with methylene chloride, washed with saturated solution of  $\text{NaHCO}_3$  and water, dried with magnesium sulphate and the solvent was then removed. Recrystallization from hot ethanol afforded 0.17 g (0.7 mmol, yield 70%) of pure benzo[1,2-*b*;4,3-*b'*] -2-nitrodithiophene; m.p.  $118\text{--}120^\circ\text{C}$ . IR (KBr,  $\text{cm}^{-1}$ ):  $\nu(\text{NO}_2)$  1515 and 1334.  $^1\text{H}$  NMR (DMSO- $d_6$ ): 8.01(d, 1H,  $\text{H}_{10}$ ,  $J = 5.2 \text{ Hz}$ ), 8.05(d, 1H,  $\text{H}_7$ ,  $J = 8.8 \text{ Hz}$ ), 8.15(d, 1H,  $\text{H}_{11}$ ,  $J = 5.2 \text{ Hz}$ ), 8.29(d, 1H,  $\text{H}_6$ ,  $J = 8.8 \text{ Hz}$ ), 8.94(s, 1H,  $\text{H}_3$ ).  $^{13}\text{C}$  NMR (DMSO- $d_6$ ): 118.62( $\text{C}_6$ ), 122.40( $\text{C}_2$ ), 124.43( $\text{C}_7$ ), 124.55( $\text{C}_{10}$ ), 129.53( $\text{C}_5$ ), 131.62( $\text{C}_5$ ), 136.66( $\text{C}_8$ ), 137.90( $\text{C}_9$ ), 138.03( $\text{C}_4$ ), 148.17( $\text{C}_{11}$ ). Anal. Calc. for  $\text{C}_{11}\text{H}_5\text{NS}_2$ : C, 51.05; H, 2.14; N, 5.95; S, 27.26. Found: C, 50.73; H, 1.95; N, 5.73; S, 28.66%.

### 4.3. Synthesis of the complexes

#### 4.3.1. Preparation of $[\text{M}(\eta^5\text{-C}_5\text{H}_5)(\text{LL})(\text{NCR})][\text{PF}_6]$

Complexes  $[\text{M}(\eta^5\text{-C}_5\text{H}_5)(\text{LL})(\text{NCR})][\text{PF}_6]$  were prepared by halide abstraction from the parent neutral complexes  $[\text{M}(\eta^5\text{-C}_5\text{H}_5)(\text{LL})\text{X}]$  (1 mmol) with  $\text{TiPF}_6$  (1 mmol) in acetone, in the presence of a slight excess (1.1 mmol), of the ligands, benzo[1,2-*b*;4,3-*b'*]dithiophen-2-carbonitrile **L1** or benzo[1,2-*b*;4,3-*b'*]dithiophen-2'-nitro-2-carbonitrile (**L2**) at reflux for 16 h under inert atmosphere. After cooling to room temperature, filtering and removing the solvent, the complexes were washed with *n*-hexane ( $3 \times 15 \text{ mL}$ ) and recrystallized from acetone/*n*-heptane or *n*-hexane, giving crystalline products.

#### 4.3.2. $[\text{Ru}(\eta^5\text{-C}_5\text{H}_5)(\text{PPh}_3)_2(\text{NCC}_{10}\text{H}_5\text{S}_2)][\text{PF}_6]$ (**1Ru**)

Orange; recrystallized from  $(\text{CH}_3)_2\text{CO}/(n\text{-heptane})$ ; 77% yield; m.p. decomposes at  $\approx 160^\circ\text{C}$ ; IR (KBr,  $\text{cm}^{-1}$ ):  $\nu(\text{CN})$  2214,  $\nu(\text{PF}_6^-)$  840;  $^1\text{H}$  NMR (DMSO- $d_6$ ): 4.75(s, 5H,  $\eta^5\text{-C}_5\text{H}_5$ ), 7.13(m, 12H,  $\text{C}_6\text{H}_5$ ,  $\text{PPh}_3$ ), 7.36(m, 12H,  $\text{C}_6\text{H}_5$ ,  $\text{PPh}_3$ ), 7.46(m, 6H,  $\text{C}_6\text{H}_5$ ,  $\text{PPh}_3$ ), 8.06(d, 1H,  $\text{H}_{10}$ ,  $J = 5.6 \text{ Hz}$ ), 8.09(d, 1H,  $\text{H}_7$ ,  $J = 8.9 \text{ Hz}$ ), 8.12(d, 1H,  $\text{H}_{11}$ ,  $J = 5.7 \text{ Hz}$ ), 8.29(d, 1H,  $\text{H}_6$ ,  $J = 8.8 \text{ Hz}$ ), 8.58(s, 1H,  $\text{H}_3$ ).  $^{13}\text{C}$  NMR (DMSO- $d_6$ ): 84.37( $\eta^5\text{-C}_5\text{H}_5$ ), 107.74( $\text{C}_2$ ), 118.51( $\text{C}_7$ ), 122.36( $\text{C}_{10}$ ), 123.72( $\text{C}_6$ ), 124.73(CN), 128.48(CH,  $\text{PPh}_3$ ), 130.15(CH,  $\text{PPh}_3$ ), 130.39( $\text{C}_{11}$ ), 132.07( $\text{C}_9$ ), 132.91(CH,  $\text{PPh}_3$ ), 134.96( $\text{C}_q$ ,  $\text{PPh}_3$ ), 135.25( $\text{C}_4$ ), 135.39( $\text{C}_3$ ), 137.27( $\text{C}_8$ ), 138.94( $\text{C}_5$ ).  $^{31}\text{P}$  NMR (DMSO- $d_6$ ):  $-144.0$ (ht,  $^1J_{\text{P,F}} = 711.5 \text{ Hz}$ ,  $\text{PF}_6$ ), 41.6(s,  $\text{PPh}_3$ ). Anal. Calc. for  $\text{C}_{52}\text{H}_{40}\text{NS}_2\text{P}_3\text{F}_6\text{Ru}$ : C, 59.43; H, 3.84; N, 1.33; S, 6.10. Found: C, 59.83; H, 3.47; N, 1.31; S, 6.17%.

#### 4.3.3. $[\text{Ru}(\eta^5\text{-C}_5\text{H}_5)(\text{PPh}_3)_2(\text{NCC}_{10}\text{H}_5\text{S}_2)][\text{CF}_3\text{SO}_3]$ (**1Ru**)

Orange; recrystallized from  $\text{CH}_2\text{Cl}_2$ -(*n*-hexane); 73% yield; m.p.: decomposes at  $\approx 167^\circ\text{C}$ ; IR (KBr,  $\text{cm}^{-1}$ ):  $\nu(\text{CN})$  2214,  $\nu_{\text{as}}(\text{CF}_3\text{SO}_3^-)$  1253;  $^1\text{H}$  NMR (DMSO- $d_6$ ): 4.78(s, 5H,  $\eta^5\text{-C}_5\text{H}_5$ ), 7.11(m, 12H,  $\text{C}_6\text{H}_5$ ,  $\text{PPh}_3$ ), 7.30(m, 12H,  $\text{C}_6\text{H}_5$ ,  $\text{PPh}_3$ ), 7.43(m, 6H,  $\text{C}_6\text{H}_5$ ,  $\text{PPh}_3$ ), 8.02(d, 1H,  $\text{H}_{10}$ ,  $J = 5.6 \text{ Hz}$ ), 8.12(d, 1H,  $\text{H}_7$ ,  $J = 8.9 \text{ Hz}$ ), 8.19(d, 1H,  $\text{H}_{11}$ ,  $J = 5.7 \text{ Hz}$ ), 8.28(d, 1H,  $\text{H}_6$ ,  $J = 8.8 \text{ Hz}$ ), 8.64(s, 1H,  $\text{H}_3$ ).  $^{13}\text{C}$  NMR (DMSO- $d_6$ ): 84.98( $\eta^5\text{-C}_5\text{H}_5$ ), 107.80( $\text{C}_2$ ), 118.59( $\text{C}_7$ ), 122.03( $\text{C}_{10}$ ), 124.01( $\text{C}_6$ ), 124.89(CN), 128.49(CH,  $\text{PPh}_3$ ), 130.07(CH,  $\text{PPh}_3$ ), 130.51( $\text{C}_{11}$ ), 132.06( $\text{C}_9$ ), 132.91(CH,  $\text{PPh}_3$ ), 135.10( $\text{C}_q$ ,  $\text{PPh}_3$ ), 135.31( $\text{C}_4$ ), 135.41( $\text{C}_3$ ), 137.27( $\text{C}_8$ ), 138.98( $\text{C}_5$ ).  $^{31}\text{P}$  NMR (DMSO- $d_6$ ): 42.0(s,  $\text{PPh}_3$ ). Anal. Calc. for  $\text{C}_{53}\text{H}_{40}\text{NS}_2\text{P}_3\text{F}_3\text{O}_3\text{Ru}$ : C, 60.33; H, 3.82; N, 1.33. Found: C, 59.98; H, 3.47; N, 1.38%.

#### 4.3.4. $[\text{Ru}(\eta^5\text{-C}_5\text{H}_5)(\text{DPPE})(\text{NCC}_{10}\text{H}_5\text{S}_2)][\text{PF}_6]$ (**2Ru**)

Yellow; recrystallized from  $(\text{CH}_3)_2\text{CO}/(n\text{-hexane})$ ; 84% yield; m.p.  $264\text{--}268^\circ\text{C}$ ; IR (KBr,  $\text{cm}^{-1}$ ):  $\nu(\text{CN})$  2216,  $\nu(\text{PF}_6^-)$  839;  $^1\text{H}$  NMR (DMSO- $d_6$ ): 2.71(m, 2H,  $-\text{CH}_2-$ ), 2.75(m, 2H,  $-\text{CH}_2-$ ), 4.99(s, 5H,  $\eta^5\text{-C}_5\text{H}_5$ ), 7.41(m, 4H,  $\text{C}_6\text{H}_5$ , DPPE), 7.59(s, 1H,  $\text{H}_3$ ), 7.60(m, 12H,  $\text{C}_6\text{H}_5$ , DPPE), 7.86(d, 1H,  $\text{H}_{10}$ ,  $J = 5.6 \text{ Hz}$ ), 7.93(d, 1H,  $\text{H}_7$ ,  $J = 8.8 \text{ Hz}$ ), 7.95(m, 4H,  $\text{C}_6\text{H}_5$ , DPPE), 8.07(d, 1H,  $\text{H}_{11}$ ,  $J = 5.6 \text{ Hz}$ ), 8.19(d, 1H,  $\text{H}_6$ ,  $J = 8.8 \text{ Hz}$ ).  $^{13}\text{C}$  NMR (DMSO- $d_6$ ): 26.99( $-\text{CH}_2-$ , DPPE), 82.42( $\eta^5\text{-C}_5\text{H}_5$ ), 107.13( $\text{C}_2$ ), 118.22( $\text{C}_7$ ), 120.36(CN), 121.96( $\text{C}_{10}$ ), 123.45( $\text{C}_6$ ), 128.90(CH, DPPE), 130.20( $\text{C}_{11}$ ), 130.71(CH, DPPE), 131.54( $\text{C}_9$ ), 132.93(CH, DPPE), 134.45( $\text{C}_3$ ), 134.51( $\text{C}_4$ ), 136.07( $\text{C}_q$ , DPPE), 137.03( $\text{C}_8$ ), 138.42( $\text{C}_5$ ).  $^{31}\text{P}$  NMR (DMSO- $d_6$ ):  $-144.0$ (ht,  $^1J_{\text{P,F}} = 711.3 \text{ Hz}$ ,  $\text{PF}_6$ ), 78.6(s, DPPE). Anal. Calc. for  $\text{C}_{42}\text{H}_{34}\text{NS}_2\text{P}_3\text{F}_6\text{Ru}$ :

C, 54.55; H, 3.71; N, 1.51; S, 6.93. Found: C, 54.42; H, 3.44; N, 1.48; S, 6.91%.

#### 4.3.5. $[Fe(\eta^5-C_5H_5)(DPPE)(NCC_{10}H_5S_2)]PF_6$ (**2Fe**)

Orange redish; recrystallized from  $(CH_3)_2CO$ -(*n*-heptane); 89% yield; m.p. decomposes at  $\approx 200$  °C; IR (KBr,  $cm^{-1}$ ):  $\nu(CN)$  2199,  $\nu(PF_6^-)$  840;  $^1H$  NMR (DMSO- $d_6$ ): 2.71(m, 2H,  $-CH_2-$ ), 2.75(m, 2H,  $-CH_2-$ ), 4.63(s, 5H,  $\eta^5-C_5H_5$ ), 7.41(m, 4H,  $C_6H_5$ , DPPE), 7.53(s, 1H,  $H_3$ ), 7.60(m, 12H,  $C_6H_5$ , DPPE), 7.87(d, 1H,  $H_{10}$ ,  $J = 5.6$  Hz), 7.94(d, 1H,  $H_7$ ,  $J = 8.8$  Hz), 7.95(m, 4H,  $C_6H_5$ , DPPE), 8.07(d, 1H,  $H_{11}$ ,  $J = 5.6$  Hz), 8.18(d, 1H,  $H_6$ ,  $J = 8.8$  Hz).  $^{13}C$  NMR (DMSO- $d_6$ ): 27.05( $CH_2$ ), 80.07( $\eta^5-C_5H_5$ ), 107.86( $C_2$ ), 118.19( $C_7$ ), 121.88( $C_{10}$ ), 123.26( $C_6$ ), 128.54(CN), 129.06(CH, DPPE), 129.96( $C_{11}$ ), 131.12(CH, DPPE), 131.51( $C_9$ ), 132.76 (CH, DPPE), 133.87( $C_3$ ), 134.42( $C_4$ ), 136.08( $C_q$ , DPPE), 136.97( $C_8$ ), 137.94( $C_5$ ).  $^{31}P$  NMR (DMSO- $d_6$ ):  $-144.1$ (qt,  $^1J_{P,F} = 710.2$  Hz,  $PF_6$ ), 96.6(s, DPPE). Anal. Calc. for  $C_{42}H_{34}NS_2P_3F_6Fe$ : C, 57.35; H, 3.90; N, 1.59; S, 7.29. Found: C, 57.07; H, 3.74; N, 1.50; S, 6.77%.

#### 4.3.6. $[Fe(\eta^5-C_5H_5)(DPPE)(NCC_{10}H_5S_2NO_2)]PF_6$ (**3Fe**)

Dark red; recrystallized from  $(CH_3)_2CO$ -(*n*-heptane); 81% yield; m.p. decomposes at  $\approx 215$  °C; IR (KBr,  $cm^{-1}$ ):  $\nu(CN)$  2197,  $\nu(NO_2)$  1517, 1329,  $\nu(PF_6^-)$  840;  $^1H$  NMR (DMSO- $d_6$ ): 2.72(m, 2H,  $-CH_2-$ ), 2.86(m, 2H,  $-CH_2-$ ), 4.76(s, 5H,  $\eta^5-C_5H_5$ ), 7.59(m, 12H,  $C_6H_5$ , DPPE), 7.66(m, 4H,  $C_6H_5$ , DPPE), 7.83(s, 1H,  $H_3$ ), 8.12(m, 4H,  $C_6H_5$ , DPPE), 8.18(d, 1H,  $H_6$ ,  $J = 8.8$  Hz), 8.24(d, 1H,  $H_7$ ,  $J = 8.8$  Hz), 8.71(s, 1H,  $H_{10}$ ).  $^{13}C$  NMR (DMSO- $d_6$ ): 27.23( $-CH_2-$ , DPPE), 80.36( $\eta^5-C_5H_5$ ), 110.57( $C_2$ ), 123.57( $C_6$ ), 124.68( $C_7$ ), 125.49( $C_{10}$ ), 128.76(CN), 129.12(CH, DPPE), 131.22(CH, DPPE), 132.02( $C_5$ ), 132.37 (CH, DPPE), 134.58( $C_3$ ), 134.82( $C_8$ ), 135.97( $C_q$ , DPPE), 139.10( $C_4$ ), 140.39( $C_9$ ) 151.92( $C_{11}$ ).  $^{31}P$  NMR (DMSO- $d_6$ ):  $-144.07$ (ht,  $^1J_{P,F} = 710.5$  Hz,  $PF_6$ ),

96.38(s, DPPE). Anal. Calc. for  $C_{42}H_{33}N_2O_2S_2P_3F_6Fe$ : C, 54.56; H, 3.60; N, 3.03; S, 6.93. Found: C, 54.74; H, 3.83; N, 2.94; S, 5.29%.

#### 4.3.7. $[Ru(\eta^5-C_5H_5)(TMEDA)(NCC_{10}H_5S_2)]PF_6$ (**4Ru**)

Yellow; recrystallized from  $(CH_3)_2CO$ -(*n*-heptane); 70% yield; m.p. decomposes at  $\approx 140$  °C; IR (KBr,  $cm^{-1}$ ):  $\nu(CN)$  2195,  $\nu(PF_6^-)$  840;  $^1H$  NMR (DMSO- $d_6$ ): 2.53(m, 2H,  $-CH_2-$ ), 2.63(m, 2H,  $-CH_2-$ ), 2.87(s, 6H,  $NCH_3$ ), 3.15(s, 6H,  $NCH_3$ ), 4.54(s, 5H,  $\eta^5-C_5H_5$ ), 8.05(2d, 2H,  $H_{10}$ ,  $H_{11}$ ,  $J = 5.6$  Hz), 8.12(d, 1H,  $H_7$ ,  $J = 8.8$  Hz), 8.25(d, 1H,  $H_6$ ,  $J = 8.8$  Hz), 8.94(s, 1H).  $^{13}C$  NMR (DMSO- $d_6$ ): 59.88( $NCH_3$ ), 59.88( $NCH_3$ ), 62.15( $-CH_2-$ ), 74.14( $\eta^5-C_5H_5$ ), 107.92( $C_2$ ), 114.80(CN), 118.52( $C_7$ ), 122.46( $C_{10}$ ), 123.11( $C_6$ ), 129.66( $C_{11}$ ), 132.53( $C_9$ ), 134.79( $C_3$ ), 135.07( $C_4$ ), 137.06( $C_8$ ), 138.58( $C_5$ ).  $^{31}P$  NMR (DMSO- $d_6$ ):  $-144.1$ (qt,  $^1J_{P,F} = 711.5$  Hz,  $PF_6$ ). Anal. Calc. for  $C_{22}H_{26}N_3S_2PF_6Ru$ : C, 41.12; H, 4.08; N, 6.54; S, 9.98 (error due to the instability of the compound). Found: C, 39.07; H, 3.26; N, 6.22; S, 9.34%.

### 4.4. Electrochemical experiments

The electrochemical experiments were performed on an EG&G Princeton Applied Research Model 273A potentiostat/galvanostat and monitored with a personal computer loaded with Electrochemistry PowerSuite v2.51 software from Princeton Applied Research. Cyclic voltammograms were obtained in 0.1 M solutions of  $[NBu_4][PF_6]$  in  $CH_2Cl_2$  or  $CH_3CN$ , using a three-electrode configuration with a platinum-disk working electrode (1.0 mm diameter) probed by a Luggin capillary connected to a silver-wire pseudo-reference electrode; a Pt wire auxiliary electrode was employed. The electrochemical experiments were performed under a  $N_2$  atmosphere at room temperature. The redox potentials of the complexes were measured in the presence of ferrocene as the internal

**Table 8**

Data collection and structure refinement parameters for **1Ru**, **1Ru**, **2Ru** and **2Fe**

Compound	<b>1Ru</b>	<b>1Ru</b>	<b>2Ru</b>	<b>2Fe</b>
Empirical formula	$C_{55}H_{45}F_6NOP_3RuS_2$	$C_{107}H_{80}Cl_2F_6N_2O_6P_4Ru_2S_6$	$C_{42}H_{34}F_6NP_3RuS_2$	$C_{45}H_{40}F_6FeNO_{1.33}P_3S_2$
Formula weight	1108.02	2193.01	924.80	942.99
Temperature (K)	293(2)	150(2)	293(2)	150(1)
Wavelength (Å)	1.54180	0.71073	1.54180	0.71073
Crystal system	Triclinic	Triclinic	Monoclinic	Monoclinic
Space group	$P\bar{1}$	$P\bar{1}$	$P2_1/n$	$P2_1/n$
Unit cell dimensions				
<i>a</i> (Å)	13.415(7)	12.281(2)	11.370(3)	9.2211(5)
<i>b</i> (Å)	14.763(8)	13.550(3)	14.984(3)	19.5890(13)
<i>c</i> (Å)	17.049(8)	33.005(7)	23.765(5)	23.4609(15)
$\alpha$ (°)	69.02(2)	82.619(6)	–	–
$\beta$ (°)	87.87(2)	84.873(7)	102.25(2)	93.240(2)
$\gamma$ (°)	65.49(3)	63.176(6)	–	–
Volume (Å <sup>3</sup> )	2844(3)	4858(2)	3957(2)	4231.0(5)
Z	2	2	4	4
Calculated density (Mg m <sup>-3</sup> )	1.294	1.499	1.553	1.480
Absorption coefficient (mm <sup>-1</sup> )	4.186	0.630	5.868	0.633
<i>F</i> (000)	1130	2232	1872	1939
$\theta$ Range for data collection (°)	3.55–66.92	1.86–28.61	3.51–66.93	2.03–20.61
Limiting indices	$-15 \leq h \leq 16$ $-16 \leq k \leq 16$ $0 \leq l \leq 20$	$-16 \leq h \leq 12$ $-18 \leq k \leq 18$ $-44 \leq l \leq 42$	$-13 \leq h \leq 0$ $-17 \leq k \leq 0$ $-18 \leq l \leq 28$	$-9 \leq h \leq 9$ $-19 \leq k \leq 19$ $-23 \leq l \leq 23$
Reflections collected/unique	9756/9756	57,369/24,723	6959/6665	33,367/4296
$[R_{int}]$	[0.0000]	[0.0823]	[0.1491]	[0.0728]
Completeness to $\theta$	66.92 (96.4%)	28.61 (99.2%)	66.93 (94.5%)	20.61 (99.6%)
Refinement method	Full-matrix least-squares on $F^2$	Full-matrix least-squares on $F^2$	Full-matrix least-squares on $F^2$	Full-matrix least-squares on $F^2$
Data/restraints/parameters	9756/0/623	24,723/4/1217	6665/0/497	4296/0/536
Goodness-of-fit on $F^2$	1.095	0.913	1.045	1.181
Final <i>R</i> indices [ $I > 2\sigma(I)$ ]	$R_1 = 0.0930$ ; $wR_2 = 0.2363$	$R_1 = 0.0738$ ; $wR_2 = 0.2010$	$R_1 = 0.0624$ ; $wR_2 = 0.1665$	$R_1 = 0.0338$ ; $wR_2 = 0.0897$
Extinction coefficient	0.0100(7)	–	0.00067(11)	–
Largest difference in peak and hole (e Å <sup>-3</sup> )	1.831 and $-1.488$	2.169 and $-1.543$	1.390 and $-2.248$	0.461 and $-0.429$

standard and the redox potential values are normally quoted relative to the SCE by using the ferrocenium/ferrocene redox couple ( $E_{p/2} = 0.46$  or  $0.40$  V vs. SCE for  $\text{CH}_2\text{Cl}_2$  or  $\text{CH}_3\text{CN}$ , respectively) [49].

The supporting electrolyte was purchased from Aldrich Chemical Co., recrystallized from ethanol, washed with diethyl ether and dried under vacuum at  $110^\circ\text{C}$  for 24 h. Reagent grade acetonitrile and dichloromethane were dried over  $\text{P}_2\text{O}_5$  and  $\text{CaH}_2$ , respectively, and distilled under nitrogen atmosphere before use.

#### 4.5. Crystal structure determination

X-ray data were collected on a TURBOCAD4 Enraf–Nonius diffractometer with a rotating anode and  $\text{Cu K}\alpha 1$  radiation ( $\lambda = 1.5418\text{\AA}$ ), at room temperature for compounds **1Ru** and **2Ru**. Data were corrected for Lorentz and polarization effects and for absorption by XABS2 empirical method (included in WINGX-version 1.70.01 [50]) for compound **1Ru** and by semiempirical methods based on  $w$ -scans [51] for compound **2Ru**. Data collection and data reduction were done with CAD4 and XCAD programs [52].

For compounds **1Ru** and **2Fe** x-ray data were collected on a Bruker AXS APEX CCD area detector diffractometer at  $150(1)\text{K}$  using graphite-monochromated  $\text{MoK}\alpha$  ( $\lambda = 0.71073\text{\AA}$ ) radiation. Intensity data were corrected for Lorentz polarization effects. Empirical absorption correction using SADABS [53] was applied and the data reduction was done with SMART and SAINT programs [54].

All structures were solved by direct methods with SIR97 [55] and refined by full-matrix least-squares on  $F^2$  with SHELXL97 [56], both included in the package of programs WINGX-version 1.70.01 [36]. Non-hydrogen atoms were refined with anisotropic thermal parameters whereas H-atoms were placed in idealised positions and allowed to refine riding on the parent C atom. Graphical representations were prepared using ORTEP [57] and MERCURY 1.1.2 [58]. A summary of the crystal data, structure solution and refinement parameters are given on Table 8.

#### 4.6. Second harmonic generation (SHG)

The measurements at a wavelength of  $1500\text{ nm}$  were carried out as described in [41]. Instead of the third harmonic ( $355\text{ nm}$ ) generated by an Nd:YAG laser with a wavelength of  $1064\text{ nm}$ , the optical parametric oscillator (OPO) in use was pumped with the second harmonic ( $532\text{ nm}$ ). The signal intensity at  $824\text{ nm}$  and the fundamental at  $532\text{ nm}$  were removed from the Idler using dichroic mirrors (HR 650–850 and HR 532), green light and a silicon filter (transparent  $>1000\text{ nm}$ ). An additional Glan–Taylor polarizer ensured the vertical polarization of the beam in the measurement cell. Measurements were performed with  $10^{-4}$ – $10^{-6}\text{ M}$  solutions. The validity of Beer law was confirmed by UV–Vis measurements of samples with corresponding concentrations. Disperse Red 1 (DR 1) was used as an external standard with a value of  $\beta_{1500}(\text{DR1}) = 70 \times 10^{-30}\text{ esu}$ . This value was obtained by comparing the slopes of the reference in  $\text{CH}_2\text{Cl}_2$  and  $\text{CHCl}_3$  to obtain the ratio of  $\beta_{\text{solute}}$  [44]. Using the value  $\beta_{1500}(\text{CHCl}_3) = 80 \times 10^{-30}\text{ esu}$  [46], the hyperpolarizability of DR 1 in  $\text{CH}_2\text{Cl}_2$  is estimated to be  $70 \times 10^{-30}\text{ esu}$ . The effect of the refractive indices of the solvents was corrected using the simple Lorentz local field [59]. The measurements were carried out with  $\text{CH}_2\text{Cl}_2$  solutions with a starting concentration of  $1.25 \times 10^{-3}\text{ M}$  for **2Fe**,  $1.89 \times 10^{-3}\text{ M}$  for **2Ru** and  $3.24 \times 10^{-3}\text{ M}$  for **3Fe**.

#### Acknowledgements

Fundação para a Ciência e Tecnologia is acknowledged for financial support (POCTI/QUI/48433/2002). Pedro Florindo thanks FCT for his Ph.D Grant (SFRH/BD/12432/2003).

E. Licandro acknowledge joint financial support from the Ministero dell'Istruzione, dell'Università e della Ricerca Scientifica (MUR), Rome, and the University of Milan (FIRB project, Bando 2003, Progetto RBNE033KMA, title of the project: "Molecular compounds and hybrid nanostructured materials with resonant and non resonant optical properties for photonic devices."

#### Appendix A. Supplementary material

CCDC 683038, 683039, 683041 and 683040 contain the supplementary crystallographic data for this paper. These data can be obtained free of charge from The Cambridge Crystallographic Data Centre via [www.ccdc.cam.ac.uk/data\\_request/cif](http://www.ccdc.cam.ac.uk/data_request/cif). Supplementary data associated with this article can be found, in the online version, at [doi:10.1016/j.jorganchem.2008.05.035](https://doi.org/10.1016/j.jorganchem.2008.05.035).

#### References

- [1] H.S. Nalwa, Appl. Organomet. Chem. 5 (1991) 349.
- [2] N.J. Long, Angew. Chem. Int. Ed. Engl. 34 (1995) 21.
- [3] S.R. Marder, in: D.W. Bruce, D. O'Hare (Eds.), Inorganic Materials, second ed., Wiley, Chichester, 1996, p. 121.
- [4] I.R. Whittall, A.M. McDonagh, M.G. Humphrey, M. Samoc, Adv. Organomet. Chem. 42 (1998) 291.
- [5] E. Goovaerts, W.E. Wenseleers, M.H. Garcia, G.H. Cross, in: H.S. Nalwa (Ed.), Handbook of Advanced Electronic and Photonic Materials, vol. 9, 2001, p. 127 (Chapter 3).
- [6] S. Di Bella, Chem. Soc. Rev. 30 (2001) 355.
- [7] A.R. Dias, M.H. Garcia, M.P. Robalo, M.L.H. Green, K.K. Lai, A.J. Pulham, S.M. Klueber, G. Balavoine, J. Organomet. Chem. 453 (1993) 241.
- [8] A.R. Dias, M.H. Garcia, J.C. Rodrigues, M.L.H. Green, S.M. Kuebler, J. Organomet. Chem. 475 (1994) 241.
- [9] M.H. Garcia, M.P. Robalo, A.R. Dias, M.F.M. Piedade, A. Galvão, M.T. Duarte, W. Wenseleers, E. Goovaerts, J. Organomet. Chem. 619 (2001) 252.
- [10] W. Wenseleers, A.W. Gerbrandtj, E. Goovaerts, M.H. Garcia, M. Paula Robalo, Paulo J. Mendes, João C. Rodrigues, A.R. Dias, J. Mater. Chem. 8 (1998) 925.
- [11] M.H. Garcia, M.P. Robalo, A.R. Dias, M.T. Duarte, W. Wenseleers, G. Aerts, E. Goovaerts, M.P. Cifuentes, S. Hurst, M.G. Humphrey, M. Samoc, B. Luther-Davies, Organometallics 21 (2002) 2107.
- [12] I.R. Whittall, M.G. Humphrey, A. Persoons, S. Houbrechts, Organometallics 15 (1996) 1935.
- [13] I.R. Whittall, M.P. Cifuentes, M.G. Humphrey, B. Luther-Davies, M. Samoc, S. Houbrechts, A. Persoons, G.A. Heath, D.C.R. Hockless, J. Organomet. Chem. 549 (1998) 127.
- [14] I.-Y. Wu, J.T. Lin, J. Luo, C.-S. Li, C. Tsai, Y.S. Wen, C.-C. Hsu, F.-F. Yeh, L. Sean, Organometallics 17 (1998) 188.
- [15] M.H. Garcia, P.J. Mendes, M.P. Robalo, A.R. Dias, J. Campo, W. Wenseleers, E. Goovaerts, J. Organomet. Chem. 692 (2007) 3027.
- [16] J.L. Oudar, H. Leperson, Opt. Commun. 15 (1975) 258.
- [17] A. Dulcic, C. Flytzanis, C.L. Tang, D. Pepin, M. Fetizon, Y. Hoppilliard, J. Chem. Phys. 74 (1981) 1559.
- [18] M. Ciofalo, G. La Manna, Chem. Phys. Lett. 263 (1996) 73.
- [19] T.L. Porter, D. Minore, D. Zhang, J. Phys. Chem. 99 (1995) 13213.
- [20] R.D.A. Hudson, A.R. Manning, D.F. Nolan, I. Asselberghs, R. Van Boxel, A. Persoons, J.F. Gallagher, J. Organomet. Chem. 619 (2001) 141.
- [21] R.D.A. Hudson, I. Asselberghs, K. Clays, L.P. Cuffe, J.F. Gallagher, A.R. Manning, A. Persoons, K. Wostyn, J. Organomet. Chem. 435 (2001) 637.
- [22] M.H. Garcia, S. Royer, M.P. Robalo, A.R. Dias, J.-P. Tranchier, R. Chavignon, D. Prim, A. Auffrant, F. Rose-Munch, E. Rose, J. Vaissermann, A. Persoons, I. Asselberghs, Eur. J. Inorg. Chem. (2003) 3895.
- [23] B. Insuasty, C. Atienza, C. Seoane, N. Martín, J. Garin, J. Orduna, R. Alcalá, B. Villacampa, J. Org. Chem. 69 (2004) 6986.
- [24] J.-L. Fillaut, J. Perruchon, P. Blanchard, J. Roncali, S. Golhen, M. Allain, A. Migalska-Zalas, I.V. Kityk, B. Sahrhoui, Organometallics 24 (2005) 687.
- [25] Y. Liao, B.E. Eichinger, K.A. Firestone, M. Haller, J. Luo, W. Kaminsky, J.B. Benedict, P.J. Reid, A. K-Y Jen, L.R. Dalton, B.H. Robinson, J. Am. Chem. Soc. 127 (2005) 2758.
- [26] A.-L. Roy, M. Chavarot, E. Rose, F. Rose-Munch, A.-J. Attias, D. Kréher, J.-L. Fave, C. Kamierszky, C.R. Chimie 8 (2005) 1256.
- [27] J.C. Calabrese, L.T. Cheng, J.C. Green, S.R. Marder, W. Tam, J. Am. Chem. Soc. 113 (1991) 7227.
- [28] S. Maiorana, A. Papagni, E. Licandro, R. Annunziata, P. Paravidino, D. Perdicchia, C. Giannini, K. Clays, A. Persoons, Tetrahedron 59 (2003) 6481.
- [29] P. Florindo, Ph.D. Thesis, University of Lisbon, Faculty of Sciences, 2008.
- [30] R.L. Cordiner, D. Albesa-Jové, R.L. Roberts, J.D. Farmer, H. Puschmann, D. Corcoran, A.E. Goeta, J.A.K. Howard, P.J. Low, J. Organomet. Chem. 690 (2005) 4908.
- [31] R.L. Cordiner, D. Corcoran, D.S. Yufit, A.E. Goeta, J.A.K. Howard, P.J. Low, Dalton Trans. (2003) 3541.

- [32] M.T. Duarte, M.F.M. Piedade, M.P. Robalo, C. Jacob, M.H. Garcia, *Acta Cryst.* C62 (2006) m531.
- [33] W. Wenseleers, E. Goovaerts, P. Hepp, M.H. Garcia, M.P. Robalo, A.R. Dias, M.F.M. Piedade, M.T. Duarte, *Chem. Phys. Lett.* 367 (2003) 390.
- [34] F.H. Allen, *Acta Cryst.* B58 (2002) 380.
- [35] G.A. Jeffrey, *An Introduction to Hydrogen Bonding*, Oxford University Press, 1997.
- [36] K.E. Maly, E. Gagnon, T. Maris, J.D. Wuest, *J. Am. Chem. Soc.* 129 (2007) 4306.
- [37] X. Lin, J. Jia, X. Zhao, K.M. Thomas, A.J. Blake, G.S. Walker, N.R. Champness, P. Hubberstey, M. Schröder, *Angew. Chem. Int. Ed.* 45 (2006) 7358.
- [38] K. Clays, A. Persoons, *Rev. Sci. Instrum.* 63 (1992) 3285.
- [39] (a) J.L. Oudar, S.S. Chemla, *Chem. Phys.* 66 (1977) 2664;  
(b) E. Hendrickx, K. Clays, C. Dehu, J.L. Brédas, *J. Am. Chem. Soc.* 117 (1995) 3547.
- [40] J.J. Wolff, R. Wortmann, *Adv. Phys. Org. Chem.* 32 (1999) 121.
- [41] S. Stadler, R. Dietrich, G. Bourhill, C. Bräuchle, A. Pawlik, W. Grahn, *Chem. Phys. Lett.* 247 (1995) 271.
- [42] Ch. Lambert, G. Nöll, E. Schmälzlin, K. Meerholz, Ch. Bräuchle, *Chem. Eur. J.* 4 (1998) 2129.
- [43] (a) K. Clays, E. Hendrickx, T. Verbiest, A. Persoons, *Adv. Mater.* 10 (1998) 643;  
(b) J.J. Wolff, R. Wortmann, *J. Prakt. Chem.* 340 (1998) 99;  
(c) S. Stadler, R. Dietrich, G. Bourhill, C. Bräuchle, *J. Phys. Chem.* 100 (1996) 6927.
- [44] T. Kodaira, A. Watanabe, O. Ito, M. Matsuda, K. Clays, A. Persoons, *J. Chem. Soc., Faraday Trans.* 93 (1997) 3039.
- [45] Z. Wu, R. Ortiz, A. Fort, M. Barzoukas, S.R. Marder, *J. Organomet. Chem.* 528 (1997) 217.
- [46] D.D. Perrin, W.L.F. Amarego, D.R. Perrin, *Purification of Laboratory Chemicals*, second ed., Pergamon, New York, 1980.
- [47] G.S. Ashby, M.I. Bruce, I.B. Tomkins, R.C. Walli, *Aust. J. Chem.* 32 (1979) 1003.
- [48] Y. Ohki, N. Uehara, H. Suzuki, *Organometallics* 22 (2003) 59.
- [49] N.G. Connelly, W.E. Geiger, *Chem. Rev.* 96 (1996) 877.
- [50] L.J. Farrugia, *J. Appl. Cryst.* 32 (1999) 837.
- [51] A.C.T. North, D.C. Phillips, F.S. Mathews, *Acta Crystallogr.* A24 (1968) 351.
- [52] K. Harms, S. Wocadlo, *XCAD4-CAD4 Data Reduction*, University of Marburg, Marburg, Germany, 1995.
- [53] *SADABS: Area-Detector Absorption Correction*, Bruker AXS Inc., Madison, WI, 2004.
- [54] *SAINT: Area-Detector Integration Software (Version7.23)*, Bruker AXS Inc, Madison, WI, 2004.
- [55] A. Altomare, M.C. Burla, M. Camalli, G. Cascarano, G. Giacovazzo, A. Guagliardi, A.G.G. Moliterni, G. Polidoro, R. Spagna, *J. Appl. Cryst.* 32 (1999) 115.
- [56] G.M. Sheldrick, *SHELXL-97: Program for the Refinement of Crystal Structure*, University of Göttingen, Germany, 1997.
- [57] L.J. Farrugia, *J. Appl. Cryst.* 30 (1997) 565.
- [58] C.F. Macrae, P.R. Edgington, P. McCabe, E. Pidcock, G.P. Shields, R. Taylor, M. Towler, J. van de Streek, *Mercury: visualization and analysis of crystal structures*, *J. Appl. Cryst.* 39 (2006) 453.
- [59] Ch. Lambert, W. Gaschler, E. Schmälzlin, K. Meerholz, Ch. Bräuchle, *J. Chem. Soc., Perkin Trans.* 2 (1999) 577.